Potential future lakes from continued glacier shrinkage in the Aosta Valley Region (Western Alps, Italy)

POTENTIAL FUTURE LAKES FROM CONTINUED GLACIER SHRINKAGE IN THE AOSTA VALLEY REGION (WESTERN ALPS, ITALY)

CRISTINA VIANI (*), HORST MACHGUTH (**, ***), CHRISTIAN HUGGEL (**), ALBERTO GODIO (****), DIEGO FRANCO (****), LUIGI PEROTTI (*), MARCO GIARDINO (*)

Affiliation

(*) Department of Earth Sciences, University of Torino, Italy

(**)Department of Geography, University of Zurich, Switzerland

(***)Department of Geosciences, University of Fribourg, Switzerland

(****) Department of Environment, Land and Infrastructure Engineering, Politecnico di Torino, Italy

Corresponding author: Cristina Viani

E-mail address: cristina.viani@unito.it

Postal address: Department of Earth Sciences - Via Valperga Caluso, 35 10125 Torino (TO), Italy

ORCID: https://orcid.org/0000-0002-0993-0509

ABSTRACT

Aosta Valley (Western Alps, Italy) is the region with the largest glacierized area of Italy. Like other high mountain regions, it has shown a significant glacier retreat starting from the end of the 'Little Ice Age' that is expected to continue in the future. As a direct consequence of glacier shrinkage, glacier-bed overdeepenings become exposed, offering suitable geomorphological conditions for glacier lakes formation. In such a densely populated and developed region, opportunities and risks connected to lakes may arise: 1) economic exploitation for hydropower production, tourism and water supply; 2) environmental relevance for high mountain biodiversity and geodiversity; 3) potential risks due to outbursts and consequent floods.

In this study, the locations of potential future glacier lakes over large glacierized areas (183 glaciers covering 163,1 km^2) of Aosta Valley were assessed by using the GlabTop2 model.

46 overdeepenings larger than 10,800 m^2 were identified, covering an area of 3.1 ± 0.9 km^2 and having a volume of 0.06 ± 0.02 km^3. The majority of the overdeepenings are located in the Monte Rosa-Cervino massif and a mean depth less than 10 m characterizes them. Moreover, an estimation of the most recent total ice volume for the Aosta Valley was provided (5.2 ± 1.6 km^3 referred to 2008).

Thanks to the validation by the proposed "backward approach" and GPR (Ground Penetrating Radar) data, we can confirm that the location of the overdeepeenings is robust while their actual dimensions are subject to considerable uncertainties. Almost all of large lakes (area > 10,000 m^2), potentially the most dangerous, are modelled. Finally, we suggest choosing medium pixel size (about 60 m) of the DEM in order to obtain, at least, the location of the largest lakes and to avoid overestimations of ice thickness and thus a great number of false positive overdeepenings.

The results presented here can be useful for understanding how the alpine environment will look like in the future and can help the management of water resources and risks related to glacier lakes.

KEY WORDS: glacier lakes; glacier shrinkage; glacier bed topography; ice thickness; Western Alps; Aosta Valley.

41 1. INTRODUCTION

42 It is expected that the rapid retreat of glaciers, observed in the European Alps and other mountain regions
43 of the world, will continue in the future (Zemp et al., 2006; IPCC, 2013, Zekollari et al., 2019). One of the
44 most evident and relevant consequences is the formation of new glacier lakes in recently deglaciated areas
45 (Linsbauer et al., 2009; Buckel et al., 2018). During glacier retreat, overdeepenings, defined by Haeberli et
46 al. (2016b) as "closed topographic depressions with adverse slopes in the flow direction, characteristic for
47 glacier beds and glacially sculpted landscapes", become exposed and, in some cases, filled with water
48 rather than sediments. Glacier-bed geomorphologic processes involved in shaping overdeepenings are
49 mainly basal sliding and bedrock abrasion by ice flux, localized bedrock quarrying and the action of complex
50 system of pressurized sub-glacial meltwater drainage (Fischer and Haeberli, 2012). The latter, in particular,
51 is supposed to play a predominant role, both in affecting basal sliding and the efficiency of direct glacier-
52 bed erosion, and in evacuating sediments keeping the bedrock accessible for further erosion (Haeberli et
53 al., 2016b).

54 Progressive shrinkage of glaciers is followed by increasing number of new glacier lakes (Paul et al. 2007;
55 Carrivick and Tweed, 2013; Mergili et al., 2013; Emmer at al., 2014; Salerno et al., 2014; Viani et al., 2016)
56 and by significant geomorphological changes (appearing/disappearing, expansion/shrinkage) in the existing
57 ones that reflect climatic fluctuations and environmental changes (Gardelle et al., 2011; Salerno et al.,
58 2014, 2016; Zhang et al., 2017).

59 When new lakes form because of glacier retreat, both opportunities and risks may arise (Haeberli et al.,
60 2016a), due to several reasons: 1) the potential economic value of glacier lakes for hydropower production,
61 tourism activities and as water reservoir (Terrier et al., 2011; Purdie, 2013; Drenkhan et al., 2019); 2) their
62 environmental relevance for high mountain biodiversity (Čiamporová-Zaťovičová and Čiampor, 2017;
63 Tiberti et al., 2019) and geodiveristy (Diolaiuti and Smiraglia, 2010); 3) the associated potential risks, e.g.
64 lake outbursts and consequent floods (Allen et al., 2009; Worni et al., 2013; Emmer et al., 2015, 2016).

65 The scientific interest and importance of these geomorphologic features is demonstrated by the high
66 number of regional glacier lake inventories produced for most of the high mountain regions of the world

since the beginning of the XXI century. The majority of the studies refers to high mountain Asia: Himalaya region (Gardelle et al., 2011; Worni et al., 2013; Zhang et al., 2015; Salerno et al., 2016), Mount Everest (Wessels et al., 2002; Bolch et al., 2008; Tartari et al., 2008; Salerno et al., 2012), Tibetan Plateau (Zhang et al., 2017), Tien Shan (Bolch et al., 2011) and Bhutan (Komori, 2008). There are also examples in South America, across the Andes (Loriaux and Casassa, 2012; Hanshaw and Bookhagen, 2014; Emmer et al., 2016; Drenkhan et al., 2018). Some studies refer to Iceland (Schomacker, 2010), Alaska (Capps and Clague, 2014) and the Caucasus (Stokes et al., 2007). Concerning the European Alps, studies were conducted in Switzerland (Huggel et al., 2002; Paul et al., 2007; Frey et al., 2010b), Austria (Emmer et al., 2015; Buckel et al., 2018) and Italy (Galluccio et al., 1998; Salerno et al., 2014; Viani et al., 2016).

More recently, the necessity has emerged of detecting and assessing suitable sites for potential glacier lakes. Several studies presented approaches for modelling location and morphometric characteristics of possible future lakes applied in some mountain regions of the world such as: Switzerland (about 500 potential new lakes modeled by Linsbauer et al., 2012); Himalaya-Karakoram (16,000 overdeepenings reported in Linsbauer et al., 2016); Peruvian Andes (201 overdeepenings identified by Colonia et al., 2017); Djungarskiy Alatau region in Central Asia (513 potential future lakes modelled by Kapitsa et al. 2017); Mont Blanc massif (80 glacier-bed overdeepenings estimated by Magnin et al., 2020).

The assessment of the potential location of future lakes is possible through ice thickness modelling and the subsequent production a of DEM (Digital Elevation Model) without glaciers (Linsbauer et al., 2009). Thereby, one assumes that future lakes form where the model predicts overdeepened areas (i.e.: overdeepenings) in the bedrock underneath existing glaciers. Results of these approaches were validated at the local scale (single glacier) through: i) the comparison of modelled ice thickness with measurements taken by *in situ* geophysical investigations (e.g., Ground Penetrating Radar), which can be logistically and economically demanding (Farinotti et al., 2017); ii) the analysis of the location of modelled overdeepenings with respect to morphological criteria (Frey et al., 2010a; Colonia et al., 2017); iii) the application of models to historical data for comparing results with the present situation (Frey et al., 2010a).

92 The goal of the present study is to assess the location of potential future lakes for the Aosta Valley Region,
93 Western Italian Alps. The area has been selected for its wide glacier extension, thus being significant for
94 providing information about future lakes (the first attempt in the Italian Alps) and adding information on
95 this topic from a newly studied region of the European Alps. The results and the suitability of the model will
96 be evaluated using further proposed ways (backward validation at the regional scale) in addition to those
97 used in existing studies (forward validation at the local scale).
98 Our specific objectives are:
99 - to give an estimation of the ice thickness and volumes of the Aosta Valley glaciers;
100 - to provide a map of possible future lakes for the region;
101 - to validate, through both well established and additional proposed ways, the suitability of the GlabTop2
102 model for modelling glacier-bed overdeepenings for mountain glaciers and for anticipating the formation of
103 lakes;
104 - to test the sensitivity of the model on the input data.
105
106 2. STUDY REGION
107 The present study focuses on the glacierized areas of the Aosta Valley Region within the Western Italian
108 Alps. The Aosta Valley is the region with the most extensive glacier cover in Italy. According to the new
109 Italian Glacier Inventory (Smiraglia et al., 2015), related to the 2005-2011 period, 192 glaciers exist in the
110 Aosta Valley Region with a cumulative area value of 133.7 km^2, which corresponds to 36% of the Italian
111 glacier area (21% with respect to the total number of glaciers). In 1991, year of the dataset used in the
112 present research, there were 183 glaciers (> 0.05 km^2) covering 163,1 km^2 (Fig. 1). The number of glaciers
113 was smaller but they covered a larger area if compared to 2005-2011. Differences in number and area are
114 due to ongoing disintegration of glaciers (from one larger, single glacier body to several smaller bodies) and
115 shrinkage and disappearance that took place in the meantime (Salvatore et al., 2015).
116 The largest glaciers, according to the 1991 dataset, were Miage (13.6 km^2), Lys (11.8 km^2) and Rutor (9.3
117 km^2).

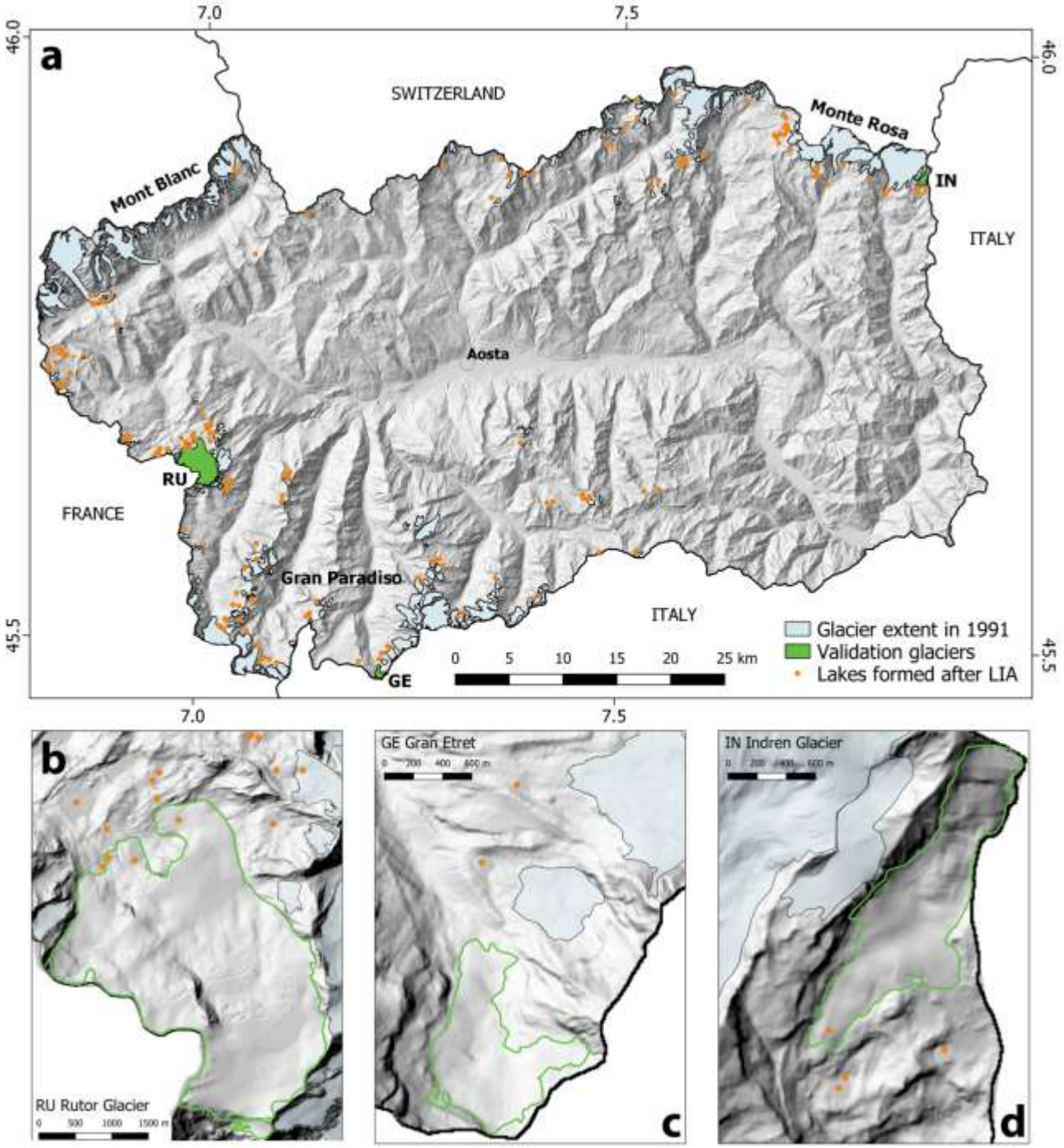

Figure 1. Map of the study region showing all Aosta Valley glaciers and all glacier lakes formed after the 'Little Ice Age' (LIA) maximum (a). Abbreviations refers to the validation glaciers shown in the detailed maps: b) Rutor (RU), c) Gran Etret (GE) and d) Indren (IN) .

The glaciers cover an elevation range from about 1400 m a.s.l. up to 4800 m a.s.l and have a mean elevation of about 3000 m a.s.l. The 15 glaciers with an area larger than 3 km^2 contribute 54% to the total

glacierized area but only 8% to the total number. On the contrary, glaciers smaller than 1 km^2 account for 80% of the number but only 23% for the area (Fig. 2). Most glaciers are mountain glaciers with few cases of valley glaciers (in 1991: Miage Glacier, Brenva Glacier, Lys Glacier, Verra Grande Glacier, Pre de Bar Glacier).

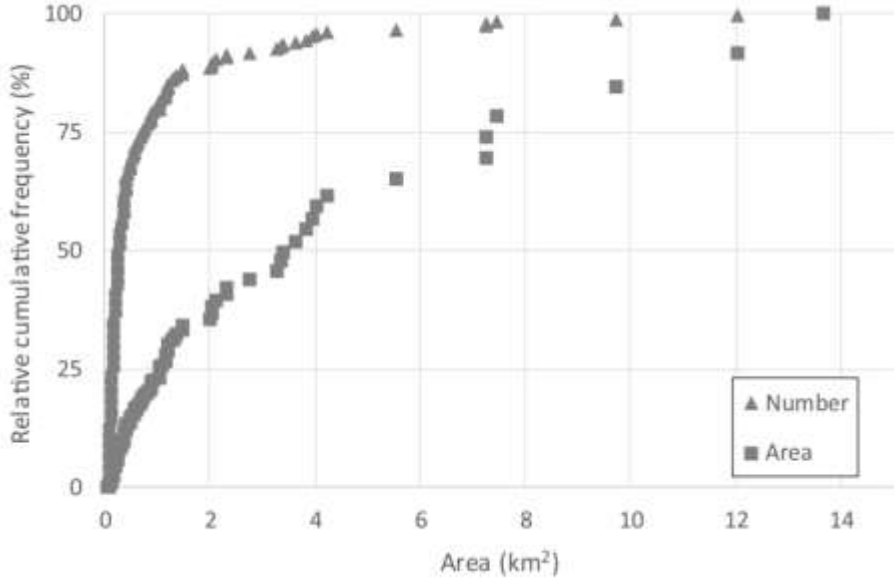

Figure 2. Plot showing the glacier area and the number of glaciers with respect to the relative cumulative frequency of both values.

Within the study region, Viani et al. (2016) reported about 200 new glacier lakes being formed within 'Little Ice Age' (LIA) glacier extent boundaries (by http://www.glariskalp.eu/ and referred to 1850. Orombelli, 2011 dated the LIA-maximum for the Western Alps in 1845-1860) covering an area of about 1.3 km^2. About ¾ of these lakes are dammed by bedrock, the remaining are mainly dammed by sediments. The 12 lakes with an area larger than 20,000 m^2 contribute 52% to the total lake coverage but only 6% to the total number. On the other hand, lakes smaller than 6,000 m^2 account for 81% of the total number, but only 23% of the total area.

Glacier lakes represent both opportunities and risks in the study region. As the Miage (Veny Valley) and Blue (Ayas Valley) lakes, some glacier lakes are important touristic attractions in addition to be valuable geosites (i.e. features showing a particular geological or geomorphological significance; Reynard, 2004). Some lakes are potentially hazardous, e.g. Rutor (Dutto and Mortara, 1992) and Miage (Diolaiuti et al.,

2006) lakes. In this context, the recent lake outburst event of August 2016 at the Gran Croux lake above Cogne (Gran Paradiso group) is mentioned (FMS, 2016).

Besides its large number of glaciers and lakes, the Aosta Valley was chosen also for its large amount of data on this topic. Information about historical (Ajassa et al., 1994; 1997; CGI-CNR, 1961; Citterio et al., 2007; Diolaiuti et al., 2012; Giardino et al., 2017) and present (Smiraglia et al., 2015; Salvatore et al., 2015) glacier extent and surface elevation are available. These data are fundamental as input data for the modelling of bedrock topography underneath glaciers and the detection of possible overdeepenings. Existing and available glacier lakes inventories (Viani, 2018) and GPR data (Villa et al., 2008) are useful for validating model results.

Three glaciers (Gran Etret, Indren and Rutor) were selected for validation of the modelled glacier bed topography with GPR data:

1) Gran Etret Glacier (0.6 km^2) is in the Gran Paradiso chain of the Graian Alps. It is a mountain glacier with a simple basin form and facing north. It lost about 75% of its LIA area (referred to 1850, http://www.glariskalp.eu/).

2) Indren Glacier (1 km^2) is a mountain glacier with a simple basin outline, facing south and located in the Monte Rosa group in the Pennine Alps. The slope is quite steep, except the central part of the glacier. The glacier front retreated about 1 km after the LIA-maximum (1850), 4 glacier lakes appeared dammed by the glacially modelled bedrock.

3) Rutor Glacier (9.1 km^2 in 1991) is located in the Rutor-Lechaud chain in the Graian Alps, facing north west. It is the third largest glacier in Aosta Valley by area and has a rather flat surface morphology. Rutor Glacier is divided into two main branches by a rocky ridge, the conjunction of the two branches is visible in the lower part of the glacier, down-valley of a rock outcrop where a medial moraine forms. The glacier has a well-known history of a series of glacier lake outburst floods between 1430 AD and 1864 AD due to front fluctuations (Orombelli, 2005). After the LIA-maximum (dated 1864 for the Rutor Glacier by Orombelli, 2005), 8 new lakes have formed dammed by moraines and in newly exposed overdeepenings (Villa et al., 2007).

169 3. DATA AND METHODS

170 Table 1 summarizes the workflow of the present research as described in the following.

STEP	INPUT DATA	METHOD
1. Modelling glacier ice thickness	Glacier outlines 1991 DEM 1991	Glacier Bed Topography Model 2 (Frey et al., 2014)
2. Calculation of bedrock topography and overdeepenings location	DEM 1991 Ice thickness distribution (raster file)	ArcGis Toolbox (Linsbauer et al., 2012)
3. Backward validation at the regional scale	Modelled overdeepenings Lake inventories (Viani, 2018)	Comparison between modelled and real lakes in areas exposed by glacier retreat between 1991 and now
4. Backward validation at the local scale	Modelled bedrock Real bedrock (LIDAR DTM 2008)	Comparison between modelled and real bedrock along selected profiles for areas exposed by the glaciers after 1991
5. Forward validation at the local scale	Modelled bedrock GPR data on specific glaciers	Comparison between modelled and measured bedrock along selected profiles
6. Forward validation at the regional scale	Modelled overdeepenings Orthophotos DEM 1991	Morphological criteria (Frey et al., 2010a)
7. Sensitivity test	DEM 1991 at different resolution	Repeat steps 1, 2, 3 and 5

171 **Table 1** - Workflow of the present research.

172

173 *3.1 The GlabTop2 model*

174 The GlabTop2 is part of the GlabTop approach (Linsbauer et al., 2009) developed for assessing the spatial
175 distribution of ice thickness by estimating the glacier depths at several points within the glaciarized areas.
176 The GlabTop approach has been widely used for modelling potential future lakes in many mountain regions
177 of the world by using recent input data (e.g. Linsbauer et al., 2016; Colonia et al., 2017; Kapitsa et al., 2017).
178 Linsbauer et al. (2012) applied GlabTop approach to historical data (glacier outlines from 1973 and a DEM
179 from 1985) for Switzerland.

The Glacier Bed Topography model version 2 (GlabTop2 model; Frey et al., 2014) is a fully automated model that requires a minimum set of input data: glacier outlines (glacier mask) and a surface DEM. It allows to model glacier bed topography over large areas combining digital terrain information and slope-related estimates of glacier thickness (Linsbauer et al., 2016). Consequently, the location of possible overdeepenings in the bedrock can be assessed.

Ice thickness *h* is calculated for an automated selection of randomly picked DEM cells within the glaciated area by using the following relationship:

$$h = \tau / (f \rho g \sin\alpha) \qquad [1]$$

τ is the basal shear stress, *f* the shape factor (related to the friction of a real glacier with the valley walls), ρ the ice density (900 kg m^{-3}), *g* the acceleration due to gravity (9.81 m s^{-2}) and α the surface slope measured over a given vertical interval (which is calculated by the model on randomly selected cells).

The calculation requires estimating the parameters τ and *f*. According to previous works (Haeberli and Hoelzle, 1995; Linsbauer et al., 2016 and Farinotti et al., 2017), τ is parameterized with the vertical extent of the entire glacier ΔH by the equation in Haeberli and Hoelzle (1995)

$$\tau = 0.005 + 1.598\Delta H - 0.435\Delta H^2 \qquad [2]$$

Following Linsbauer et al. (2012), *f* is set to 0.8 for all glaciers which is typical for valley glaciers.

The model was run using the above-mentioned parameter settings identical to the original parameters used by Frey et al. (2014). The resulting ice thickness distribution was subtracted from the corresponding surface DEM to provide the bed topography of the investigated glaciers.

Farinotti et al. (2017), in the framework of the Ice Thickness Models Intercomparison eXperiment (ITMIX), compared the results of a set of 17 different models for 21 test cases. The results obtained by the use of GlabTop2 are comparable in quality with more complex model approaches (e.g.: Farinotti et al., 2009; Huss and Farinotti, 2012). The model is limited in its ability to reproduce small-scale details and, in contrast to other models, performs poorly in modelling ice thickness of ice caps, but this is of no issue in the context of the present study.

206 *3.2 Application to all Aosta Valley glaciers*

207 We adopted the regional DEM of 1991 provided by the Regione Autonoma Valle d'Aosta (RAVA) with an
208 original spatial resolution of 10 m, produced by aerial photogrammetry. We down-sampled the DEM to 60
209 m for the calculation using the bilinear interpolation algorithm, to avoid influence of small-scale surface
210 morphologies on model outputs as suggested by Frey et al. (2014) and Farinotti et al. (2017). As glacier
211 outlines we used the .kml file available from the GlaRiskAlp Project website (http://www.glariskalp.eu) and
212 related to 1999. We modified and updated the outlines to the beginning of the 1990s, in order to have a
213 good fit with the 1991 DEM, by identifying glacier margin positions analysing the hillshade extracted from
214 the 1991 DEM and available orthophotos of 1988-89. In order to avoid inaccurate results, glaciers smaller
215 than 0.05 km^2 have been removed because they are subject to high uncertainties, as suggested by
216 Linsbauer et al. (2016). Subsequently, glacier outlines have been converted to a rasterized glacier mask
217 where all glacier grid cells receive unique IDs (one ID per glacier entity). We applied the model to all the
218 glaciers of the study region assessing, firstly, the ice thickness (step 1 in Tab. 1) and consequently the DEM
219 of the bedrock underneath glaciers (step 2 in Tab. 1). Finally, we produced a database of the modelled
220 overdeepenings (step 2 in Tab. 1) with associated morphometric parameters (area, depth, volume).
221 Finally, in order to estimate the most recent ice thickness and volume of the Aosta Valley glaciers, we
222 assumed that bed topography modelled by GlabTop2 is independent from the date of the input data (DEM
223 and glacier outlines). Ice thickness information have been obtained by subtracting the most recent regional
224 elevation model (2008 LIDAR DTM of the Aosta Valley representing recent glacier surface geometry) from
225 the modelled bedrock without glaciers (i.e. the result of the GlabTop2 application to the 1991 data) and
226 masking these results with the outlines from the most recent glacier inventory (2006-2007 glacier outlines
227 from Salvatore et al., 2015).
228
229 *3.3 The backward approach*
230 The main idea is to use historical datasets (glacier outlines and DEMs) as input data for the model. Steps 3
231 and 4, as presented in Tab. 1, synthesizes the proposed backward approach.

Our approach is based on the assumption that glacier retreat was a general trend since the year of acquisition of the historical data. From the year at which the datasets refer (data survey) until now, in areas exposed from glacier ice, new glacier lakes appeared and glacially shaped landforms become exposed. Following a backward-looking procedure, existing glacier lake and freshly exposed glacially shaped landforms can be used to verify, at the regional scale, the correspondence with modelled lakes and to validate modelled bedrock, respectively. The application of the described approach requires a lake inventory and the availability of recent elevation models. In a GIS environment we evaluate whether locations of modelled overdeepenings correspond to the location of the newly formed lakes for the areas exposed by glacier ice. This approach should allow to test if glacier lakes formation can be predicted by GlabTop2.

Ideally, data from earlier time periods would be used to maximize glacier retreat since then. For this reason, we performed preliminary tests for the production of DEMs from historical aerial photogrammetry (aerial photos stereo pairs of the 1954 aerophotogrammetric flight) on selected glaciers where significant glacier lakes have formed in bedrock overdeepenings (e.g.: Rutor and Indren glaciers). The quality of the photographs and the missing calibration certificate of the camera prevented an accurate evaluation of errors of the extracted orthophotos and DEMs. We also performed a real test with Structure for Motion (SfM) technique with the same aerial photographs from 1954 flight (Roberti et al. 2018) but the problem is that the photographs were not enough to obtain a correct and accurate SfM model to compare with the regional 1991 DEM. In addition, the potential dataset produced would only cover single glaciers.

Thus, we decided to use the 1991 DEM dataset as input data because of its consistent data quality and the wide area covered. Furthermore, glacier lake inventories related to the end of the 1990s, 2006 and 2012 (Viani, 2018) exist and can be used to check the real presence of modelled lakes at the regional scale.

Finally, at the local scale (glacier scale), focusing on areas subject to glacier retreat since the 1990s, it is possible to compare their actual topography with the modelled one along selected profiles. The regional 2008 LIDAR DTM of the Aosta Valley gives the recent topography.

3.4 The forward approach

In the existing literature (e.g. Linsbauer et al., 2012; 2016; Farinotti et al., 2017; Helfrischt et al., 2019), researchers used geophysical investigations carried out on selected glaciers to validate model results.

We adopt a similar approach by performing a forward-looking validation comparing Ground Penetrating Radar (GPR) profiles with modelled bedrock at the glacier scale (step 5 in Tab. 1). We consider several data sets: existing GPR data at Rutor and Gran Etret glaciers by Villa et al. (2008) and by Regional Agency ARPA VDA in collaboration with the Department of Environment, Land and Infrastructure Engineering (Politecnico di Torino), respectively. The data were acquired during different field campaigns (Rutor: 1996 and 2006, using a central frequency of 35 MHz; Gran Etret: 2013 by helicopter, using a main frequency of 70 MHz). A GPR survey was also carried out during summer 2016 (central frequency of 200 MHz) on the central area of Indren Glacier where GlabTop2 shows the presence of a possible subglacial overdeepening.

Moreover, the morphological criteria proposed by Frey et al. (2010a) can be used as a forward validation at the regional scale (Colonia et al., 2017). For each modelled overdeepening of the study area it is possible, using orthophotos and DEMs, to verify if the morphological characteristics at sites where overdeepenings are modelled fulfil the mentioned criteria (step 6 in Tab. 1).

3.5 Sensitivity test on input data

In addition to the previously presented modelling with 60 m spatial resolution datasets, we performed additional runs of GlabTop2 varying the pixel size of the input data (DEM and glacier mask) from high to low spatial resolution: 20 m, 40 m and 90 m (step 7 in Tab. 1). The objective is to evaluate the effect of the change of the pixel size on model results (ice thickness, bedrock geometry, total overdeepenings, depth and area), considering that GlabTop2 calculation of ice thickness is grid-based and that surface slope is derived as the average surface slope of all grid cells with a buffer of a given vertical elevation extent.

4. RESULTS

4.1 Thickness and volume of the Aosta Valley glaciers

In Figure 3 the ice thickness distribution for all Aosta Valley glaciers is shown. Ice thicknesses lower than 50 m are dominant. 78% of the glaciers have a mean ice thickness below 25 m and another 18% between 25 and 50 m.

We estimated a total ice volume of 5.2 ± 1.6 km^3, considering 30% as the uncertainity of the model as demonstrated by Linsbauer et. al. (2012). The arithmetic mean ice thickness, obtained by dividing the total volume by the total area, is about 39 m. Maximum modelled ice thickness is 214 m (Triolet Glacier).

Considering the volume of single glaciers, the 3, 9, and 27 largest glaciers (defined by volume) contained 28, 59 and 86% of the total volume, respectively. The three largest glaciers thereby are Miage (0.53 km^3) , Rutor (0.50 km^3) and Lys (0.45 km^3) glaciers. The thickest ones (considering the mean thickness) are Rutor (62 m), Tribolazione (61 m) and Pre de Bar (60 m) glaciers.

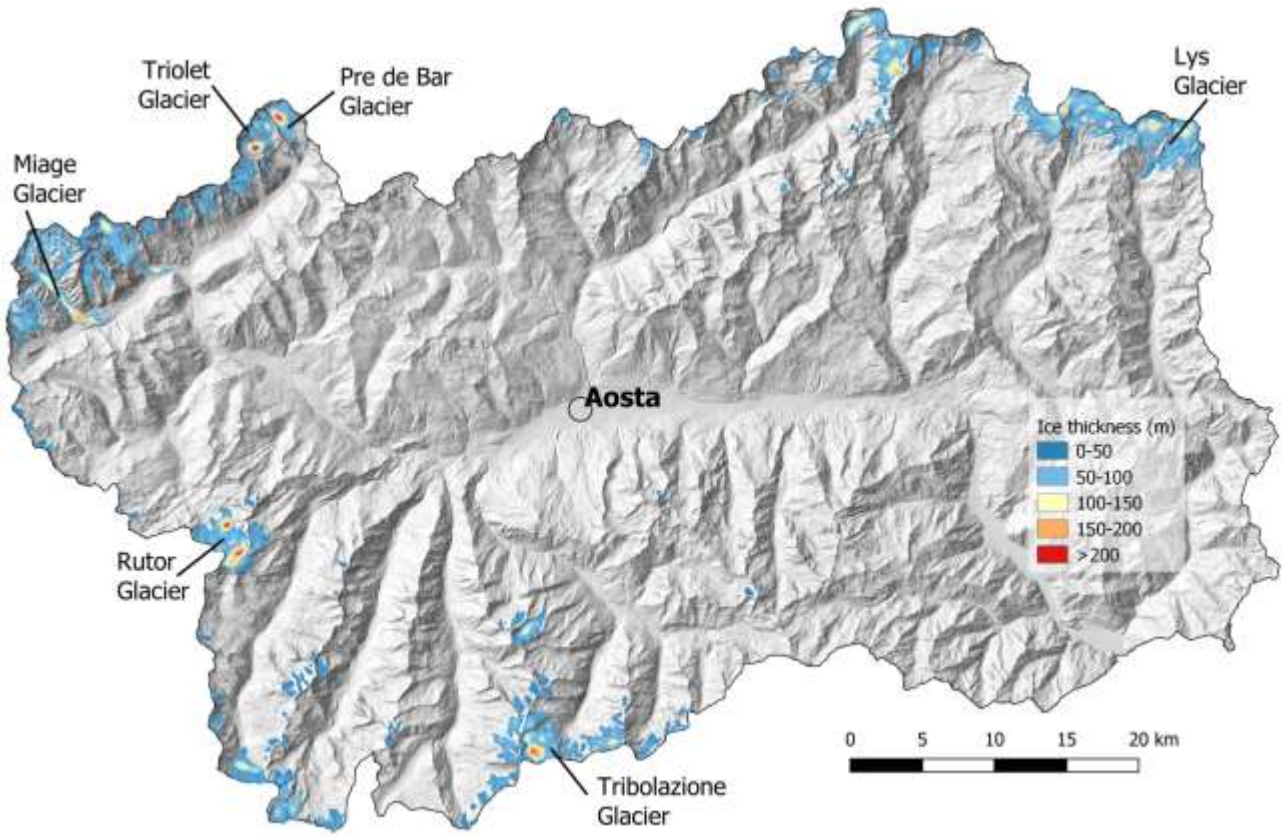

296 **Figure 3.** Ice thickness distribution for the Aosta Valley glaciers in 2008. The largest (Miage, Rutor and Lys)
297 and thickest (Rutor, Tribolazione and Pre de Bar) glaciers are indicated by their name, as well as the glacier
298 with maximum modelled ice thickness (Triolet).
299
300 *4.2 Potential future lakes*
301 The total number of detected overdeepenings is 46. We used an area threshold of 10,800 m^2 (or about 1
302 ha) for the lakes area, which means a lake resulting from 3 pixels of the 60 m spatial resolution modelling.
303 Figure 4 shows the location, mean depth and area of the overdeepenings located in the most important
304 glacierized areas of the study region. Overdeepenings are mainly located in correspondence of areas where
305 the 1991 glacier surface was flat (slope < 5°). For the steepest mountain glaciers, located for example in the
306 Mont Blanc massif, few overdeepenings have been modelled. About 3.1 ± 0.9 km^2 of potential future lakes
307 can contain a total volume of 0.06 ± 0.02 km^3, which is less than 1% of the corresponding total glacier
308 volume (7.3 km^3 in 1991). The average depth of the modelled overdeepenings is about 18 m (weighted with
309 the total area). Potential future lakes could be less deep and have smaller area and volume than the
310 modelled overdeepenings as they may not completely fill up.

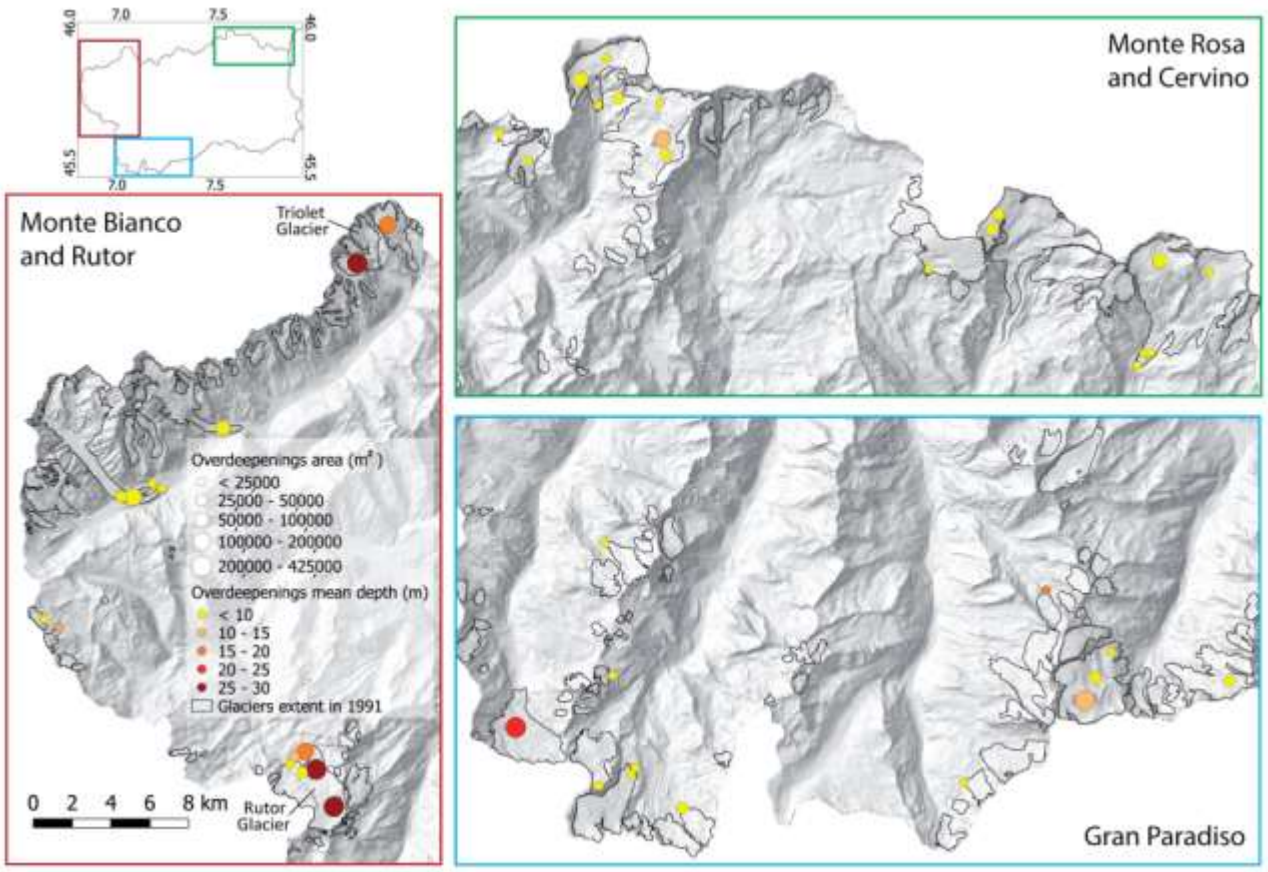

311

312 **Figure 4**. Location of modelled overdeepenings for the main massifs of the Aosta Valley Region. The size of
313 the points refers to the area of the overdeepening and the colour to the mean depth. The two glaciers
314 hosting the largest overdeepenings are indicated.

315

316 The average area of overdeepenings is 68,000 m^2 with a volume of $1.2 \cdot 10^6$ m^3. Seven modelled
317 overdeepenings larger than $1 \cdot 10^6$ m^3 account for 89% of the total volume and the two largest ones (each >
318 $10 \cdot 10^6$ m^3) for almost half (45%) of total volume. These two overdeepenings are located underneath the
319 Rutor (A = 425,000 m^2 and V = $12.6 \cdot 10^6$ m^3) and the Triolet (A = 360,000 m^2 and V = $12.2 \cdot 10^6$ m^3) glaciers
320 (Fig. 4).

321 In terms of distribution, the majority of the overdeepenings are located in the Monte Rosa-Cervino massif.
322 However, mean depths of less than 10 m characterizes them. In the Mont Blanc massif, there are few
323 overdeepenings due to morphology of the remaining glaciers that are the steepest of the study area.
324 Exceptions are Miage and Rutor glaciers that have large overdeepenings. Modelled overdeepenings are
325 mostly located at the front of the glaciers or in wide and flat accumulation areas.

4.3 Backward and regional validation

Between the 1990s and now, glaciers have retreated in the whole study region, glacially shaped landscapes became exposed and new lakes formed. For backward-looking validation, we used the overdeepenings located in areas exposed from glacier ice between the 1990s and 2012 and compared them with the actual surface topography and lakes (where they have formed).

We focused on:

- existing lakes modelled as overdeepenings by GlabTop2;
- existing lakes that have not been modelled (false negatives);
- modelled overdeepenings not corresponding to real lakes (false positives).

Over the time period 1990s to 2012, according to Viani et al. (2016), 35 lakes formed in areas exposed by glaciers. Their area varies from a minimum of 300 m^2 to a maximum of about 50,000 m^2. There are only six lakes greater than 10,000 m^2 (large lakes), seven have an area between 5,000 and 10,000 m^2 (medium lakes) and 22 are smaller than 5,000 m^2 (small lakes).

Considering model results, in the areas corresponding to glacier retreat, 16 overdeepenings (> 10,800 m^2) have been modelled.

Nine (26%) of the 35 newly formed lakes have been modelled by GlabTop2: 5 of the large lakes, 2 of the medium lakes and 2 of the small lakes, which means that almost all of the large lakes are modelled, a third of the medium ones and almost none of the smallest ones. Lowering the threshold of the minimum area of overdeepenings from 10,800 to i.e. 3,600 m^2 (that corresponds to a lake resulting from only 1 pixel of the 60 m modeling) would have permitted to model 6 more existing lakes (3 medium and 3 small) but then, more false positive (i.e. modelled overdeepenings not corresponding to real lakes) would have been produced, increasing the uncertainty of the results.

The modelled overdeepenings mostly are larger than the real lakes; this is not considered a major issue because overdeepenings containing a lake might often not get completely filled by water and/or partly filled with sediments.

352 The modelling results in 26 false negatives (i.e. existing lakes that have not been modelled): 1 large lake, 5
353 medium lakes and 20 small lakes. The largest lake (area of about 13,000 m^2), is located in the proglacial
354 area of the Rutor Glacier (L_2 in Fig. 12a) as well as one of the medium lakes (M in Fig. 12a). The majority of
355 the remaining false negatives (70%) are located at glaciers with an area smaller than 1 km^2. Moreover,
356 analysing the slope of the 1991 glacier surface at the location of the false negatives, we observe that for the
357 majority of them (73%) the slope is greater than 20°.
358 Nine of the modelled overdeepenings (56%) correspond to real lakes (Tab. 2). Analysing the remaining 7
359 ones (false positives) on orthophotos we found that all are located at glacier fronts close to the glacier
360 margins. At the location of false positives, the glacier surfaces in 1991 had a medium slope of about 11°.
361 The two largest false positives (area > 21,600 m^2) are located in the proglacial area of the Rutor Glacier (ID
362 2 and ID 5 in Tab. 2 and Fig. 12a). The remaining false positives have an area smaller than 14,400 m^2.

		Modelled overdeepenings (GlabTop2)				Observed lakes (orthophotos)	
ID	Glacier	Area (m^2)	Max depth (m)	Mean depth (m)	Volume (10^6 m^3)	Max area measured (1990s-2012)	Geomorphological observations and notes
1	Rutor	115200	33	16	1,79	52500	See Fig. 12a
2	Rutor	36000	19	12	0,42	-	Sediments
3	Lavassey	28800	11	5	0,14	18100	See Fig. 12b
4	Lys	21600	8	3	0,07	10400	
5	Rutor	21600	6	4	0,08	-	Sediments
6	Western Gran Neyron	18000	24	16	0,29	11400	See Fig. 12c
7	Lac Gelè	18000	39	26	0,47	5200	
8	Tsa de Tsan	14400	8	5	0,08	6700	See Fig. 12d
9	Punta Laurier North	14400	19	9	0,13	-	Sediments
10	Soches Tsanteleina	14400	16	9	0,13	3000	
11	Lys	14400	11	6	0,09	10200	
12	Lys	10800	9	5	0,06	3100	
13	Traversiere North	10800	17	8	0,09	-	Bedrock (Fig. 12f)
14	Monciair	10800	8	5	0,05	-	Bedrock (Fig. 12e)
15	Mont Gelè	10800	11	6	0,07	-	Sediments and/or dead ice (Fig. 5a)
16	Invergnan	10800	13	9	0,10	-	Dead ice and water ponds (Fig. 5b)

Table 2. Main morphometric parameters of modelled overdeepenings compared with the real morphologies.

We compared modelled bedrock with real bedrock topography (LIDAR DTM 2008) in the areas where overdeepenings have been modelled but no lakes had formed (i.e. false positive, figure 5). In the two examples shown in Fig. 5, the profile extracted from the LIDAR DTM represents the elevation of the debris and/or dead ice occupying the proglacial area. Measured and modelled profiles agree well in correspondence of the rocky threshold but above they diverge. The real bedrock probably contains an overdeepening (as modelled) that can't be detected, neither from the orthophotos nor from the LIDAR DTM, because it is filled with debris and/or dead ice.

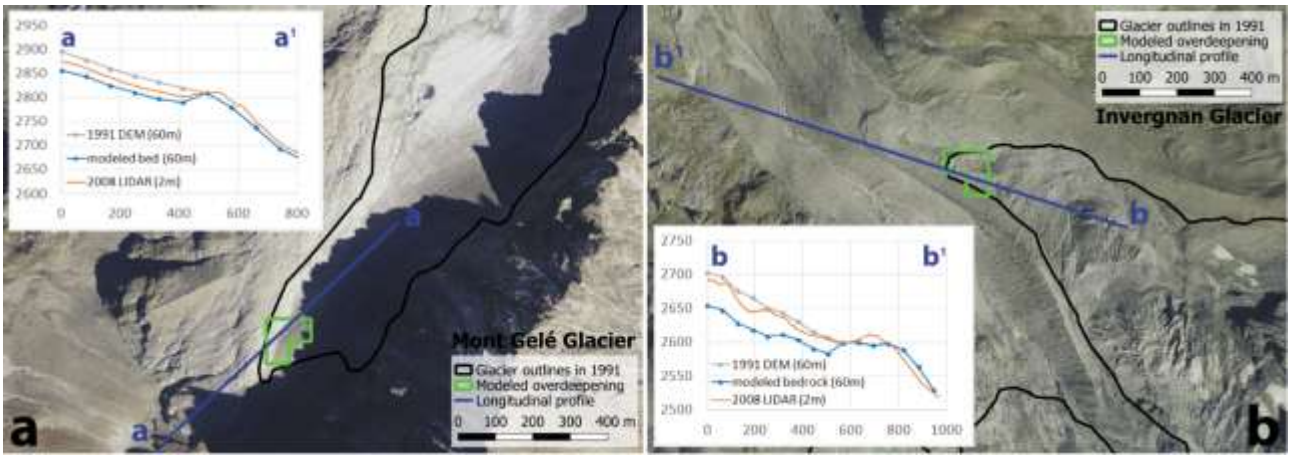

Figure 5. Comparison between modelled bedrock and real surface (LIDAR DTM 2008) for two cases (a, Mont Gelé Glacier and b, Invergnan Glacier) where an overdeepening has been modelled but no real lake exists. (Imagery: Italian National Geoportal. 2006-07 orthophotos).

4.4 Forward and local validation

We compared measured (GPR) and modelled bedrock along some profiles for the Gran Etret and Indren glaciers. In particular, we selected two cross-sectional profiles and one longitudinal profile for both glaciers (Fig. 6). We also provide a similar validation for some selected areas of the Rutor Glacier (Fig. 8).

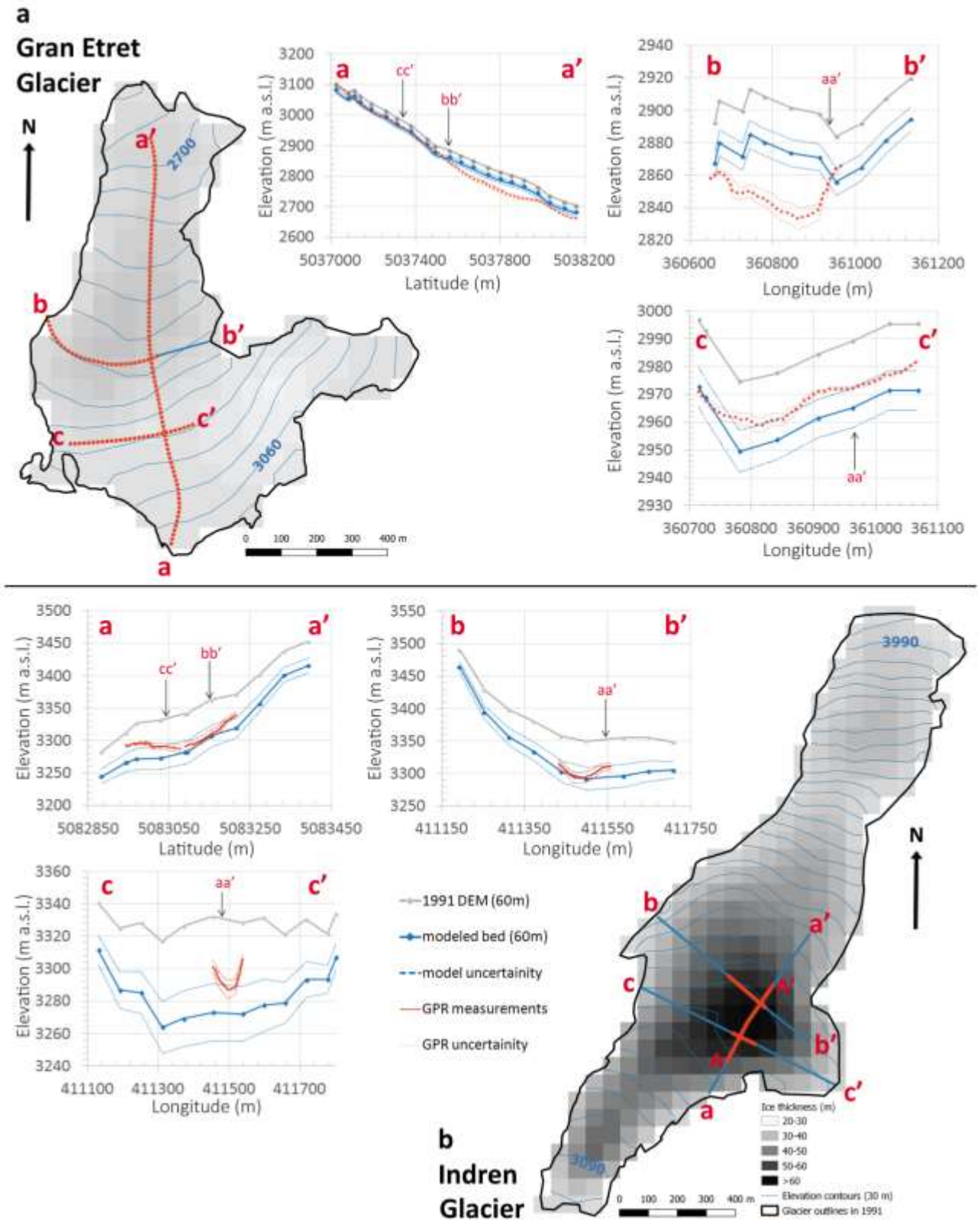

Figure 6. Maps of the modelled bedrock elevation (elevation contours) and ice thickness (grey scale grid) at Gran Etret (top left) and Indren (bottom right) glaciers. The interval of the elevation contours is 30 m a.s.l.

385 Plots show the cross-sectional and longitudinal profiles modelled with GlabTop2 and the model uncertainty
386 of ±30%, the GPR measurements and the GPR uncertainty.
387
388 In the case of Gran Etret Glacier, we noticed a good agreement between measured and modelled bedrock
389 in the highest part of the glacier, as shown for the upper part of the profile (a) and for profile (c) and the
390 deviations between measurements and model results mostly remain within the model uncertainty of ±30%.
391 The geometry of the cross sections is well captured for profile (c). On the contrary, the elevation of the
392 central part of the glacier is underestimated by the model (profiles a and b) and it is outside the uncertainty
393 range. Profile (b) shows a great difference between measured and modelled elevation values, the latter
394 underestimating the ice thickness. Considering the geometry of the cross section, the profile has similar
395 trends but the different spatial resolution of model output and GPR data as well as the short GPR track
396 prevent a good comparison.
397 At Indren Glacier, measurements and model outputs are in good agreement along the whole profile (a) and
398 (b) within the model uncertainty range. Profile (c) shows a proximity between measured and modelled
399 elevation values near the uncertainty range. It seems that the model does not capture the small U-shaped
400 geometry measured by the GPR (Fig. 6, profile cc' of the Indren Glacier, dotted red line), the divergence
401 could be due to the low spatial resolution of the model outputs.
402 The radargram corresponding to the longitudinal GPR profile AA' at Indren Glacier is shown in the following
403 Figure 7. The maximum ice thickness is measured in the central part of the profile and corresponds to
404 about 40 m.

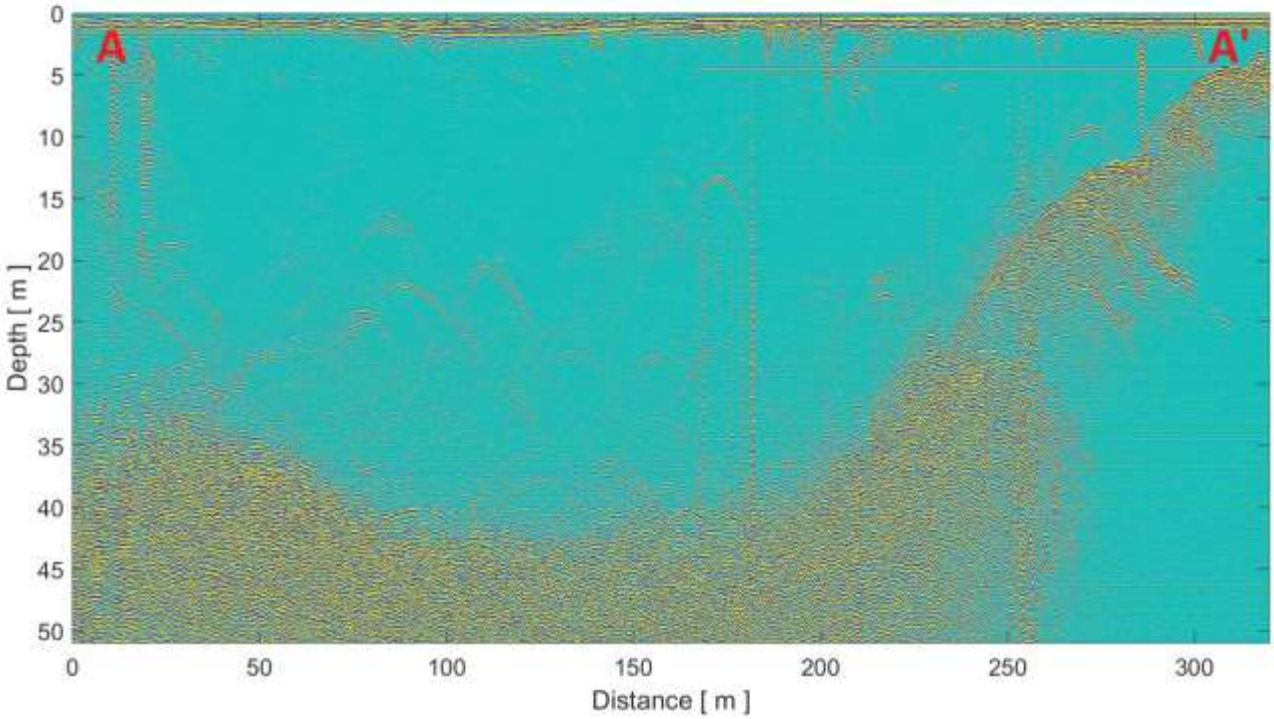

405

406 **Figure 7**. Radargram of the corresponding longitudinal GPR profile AA' at Indren Glacier.

407

408 By analysing the differences between the elevation of the bedrock measured by GPR and the one modelled
409 by Glabtop2 at Rutor Glacier (Fig. 8), a high differences between measured and modelled ice thickness is
410 observed where the model predicts overdeepenings, which corresponds to the flattest area of the glacier.
411 Maximum ice thicknesses measured by GPR at the locations of the two modelled overdeepenings is about
412 80 meters (L in Fig. 8) and 50 m (U in Fig. 8). However, comparison of the GPR data with modelled ice
413 thickness at these two overdeepenings suggests that the model overestimated the ice thickness (maximum
414 values of 229 meters in L and 203 meters in U). According to the measured profiles, small overdeepened
415 morphologies exist at the lower modelled overdeepenings, while no real overdeepened landforms exist at
416 the location of the upper modelled overdeepenings.

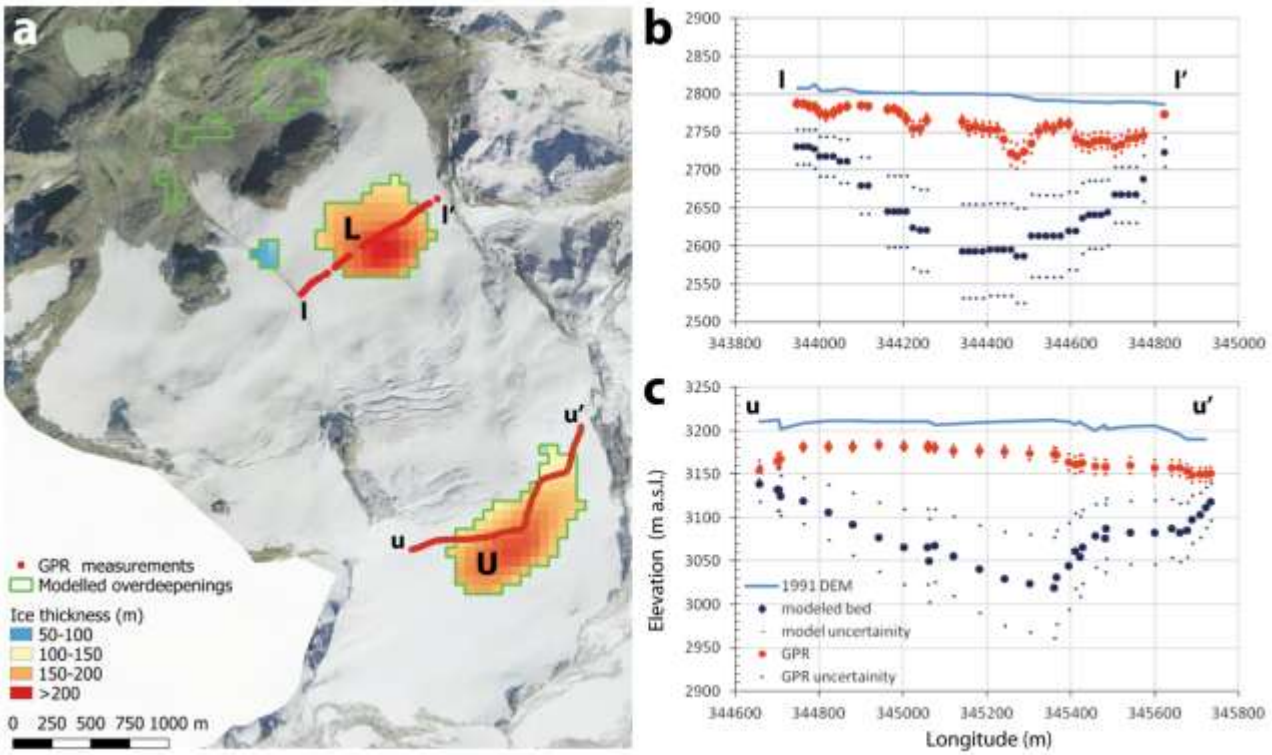

Figure 8. Maps of the two overdeepenings modelled in the lower (L) and upper (U) zone of the Rutor Glacier, corresponding ice thickness and location of GPR paths (a). Plots show the cross-sectional profiles (ll' in b and uu' in c) modelled with GlabTop2 and the model uncertainty of ±30%, the GPR measurements and the GPR uncertainty. (Imagery: Italian National Geoportal. 2006-07 orthophotos).

4.5 Sensitivity test

We performed different runs of GlabTop2, in addition to the previously presented 60 m run, varying the pixel size of the input data (DEM and glacier mask) from a high to a low spatial resolution: 20 m, 40 m and 90 m. Here we present the results related to changes in the spatial resolution of the input data. Thereby, we focused on the main parameters of the modelled overdeepenings as shown in Figure 9.

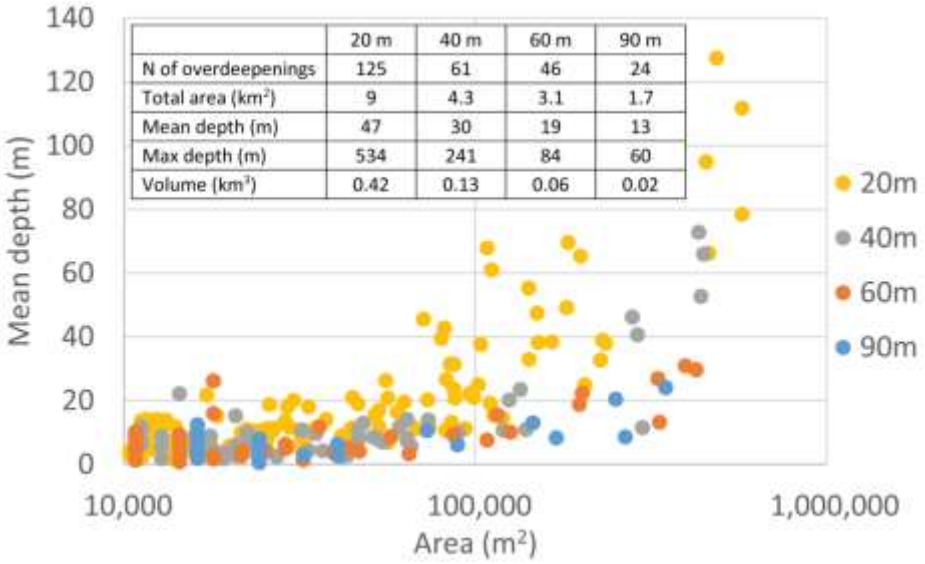

Figure 9. Scatter plot of mean depth of modelled overdeepenings versus their area as modelled for the 20 m, 40 m, 60 m and 90 m runs. The table (top left) reports the main morphometric parameters of the overdeepenings for the four different spatial resolutions.

The number of possible future lakes (surface area > 10,800 m^2) in the study area, and the total area and the total volume, varies considerably with respect to the spatial resolution of the input DEM from a minimum of 24 overdeepenings for the 90 m run to a maximum of 125 overdeepenings for the 20 m run. Focusing on Figure 9, we notice that the majority of the overdeeepenings modelled with a spatial resolution of 40, 60 and 90 m has an area lower than 100,000 m^2 and a depth lower than 20 m. Results of the 20 m run show an increase in the number, area and depth of the overdeepenings. The output of the 20 m run, with respect to the 60 m run, performs better in shaping bedrock morphologies showing a good agreement (qualitatively assessing agreement of modelled vs. measured shape) with the GPR data when we analyse the geometry of the profiles, for example, at profile b of the Gran Etret Glacier and profile c of the Indren Glacier (Figure 10). From a quantitative point of view, the results of the comparison among modelled ice thickness by 20 and 60 m runs and GPR data differ. At profile b of the Gran Etret Glacier both the 20 and 60 m run underestimated the ice thickness and the 20 m performs better. At profile c of the Indren Glacier, both the 20 and 60 m overestimated the ice thickness and the 60 m performs better.

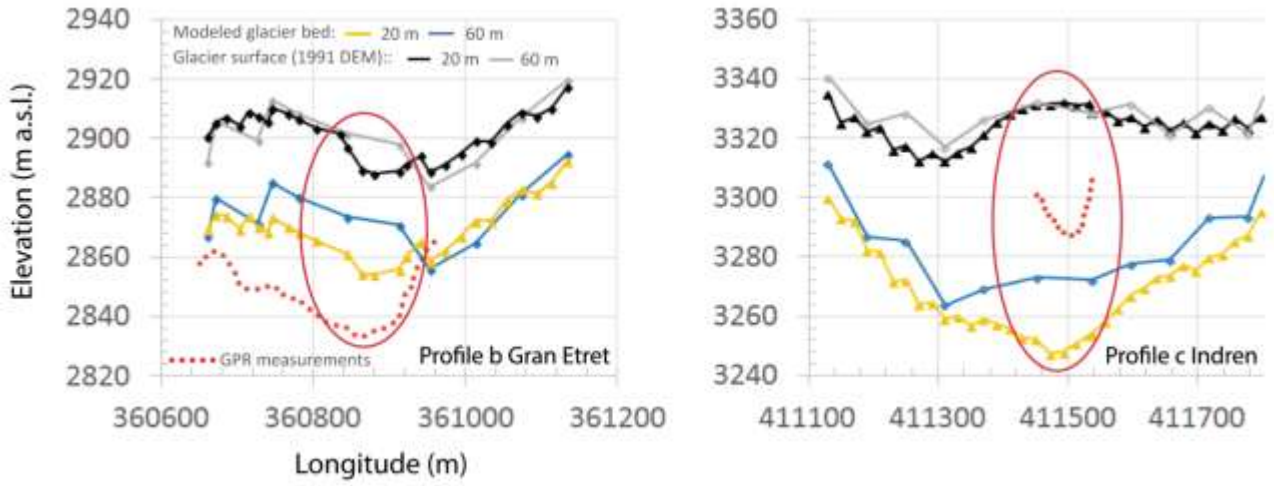

446

447 **Figure 10.** Comparison between outputs of glacier bed model using DEMs sampled to 60 m and 20 m and

448 GPR measurements along cross-sections at the Gran Etret and Indren Glacier.

449

450 Because of this divergence in the performances we decided to carry out an additional test by comparing

451 modelled overdeepenings and existing lakes for the four runs (Fig. 11). We notice that the 20 m run has the

452 highest number of modelled lakes but it is also the one with the highest number of false positive. Most of

453 them are located at glacier margins where the calculation of glacier surface slopes could be uncertain and

454 consequently results in artefacts. Modelled lakes as well as false positive decrease with the decrease of the

455 spatial resolution. Looking at the largest modelled lakes, we note that all the four runs modelled about

456 more than the 50% of the large lakes (> 10,000 m^2).

457 The 60 m run gives the best performance among the four runs in modelling large lakes (5 of the 6 lakes

458 modelled). The 20 and 40 m versions perform better than the 60 m run for small lakes and similarly to 60 m

459 run for medium lakes but false positive are the triple and the double in the 20 m and 40 m versions

460 respectively if compared to the 60 m. The 90 m run performs worst except for the small number of false

461 positives.

462 We decided to focus on the results of the 60 m run in the present work because of: 1) good performance in

463 modelling the largest lakes, potentially the most dangerous; 2) few false positive; 3) correct calculation of

464 small lakes is not demanded in the present study (considering the limited ability of the model to reproduce

465 small-scale features).

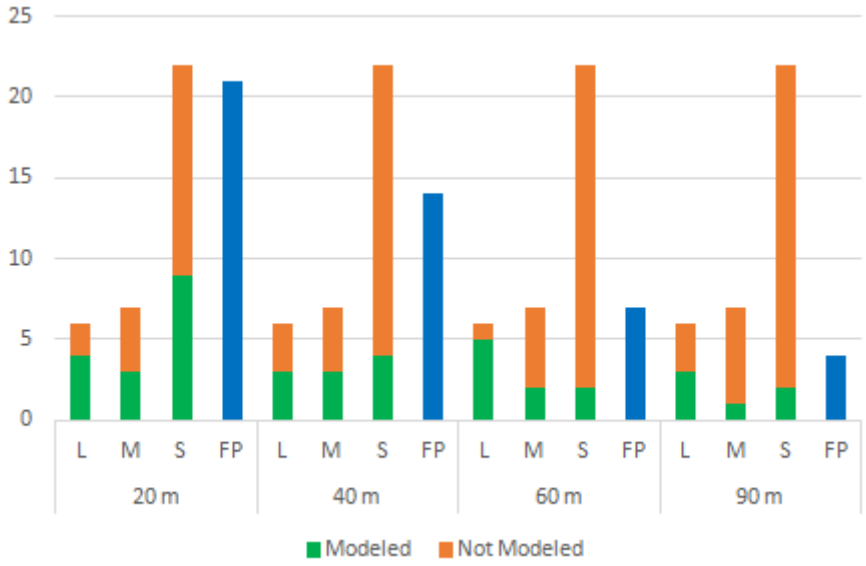

Figure 11. Model performances for the four different runs (20 m, 40 m, 60 m and 90 m); for each run the number of modelled (green) and not modelled (red) real lakes are given, differentiating among large (L, area>10,000 m^2), medium (M, area between 5,000 and 10,000 m^2) and small (S, area<5,000 m^2) existing lakes and the overdeepenings that do not correspond to real lakes (blue, false positive, FP).

5. DISCUSSION

5.1 Future landscape evolution

Within the study area, the volume of calculated potential overdeepenings (0.06 km^3) is only 0.8% of the corresponding total glacier volume (7.3 km^3 in 1991). Considering similar studies implementing GlabTop approach, we notice that the calculated value is less than the corresponding one for the Swiss Alps (3%, Linsbauer et al., 2012) and the Himalaya-Karakoram (3-4%, Linsbauer et al., 2016). However, similar values (0.5, 1%) were found for the Peruvian Andes (Colonia et al., 2017). Considering that flat areas (like valley glacier tongues) are more suitable for the modelling of overdeepenings, the higher value for the Swiss Alps can be due to the fact that the results refer to 1973 when glaciers were wider and flat tongues still existed. For the Himalaya-Karakoram the input datasets are more recent (2000-2010) and, accordingly to Bolch et al. (2012), at that stage a large part of the ice in the region was still located in the flat tongues of the valley

485 glaciers. Finally, similarity with the study of Colonia et al. (2017) in the Peruvian Andes can be due to the
486 limited extent of remaining flat glacier parts. Many Peruvian glaciers, similar to the glaciers of the Aosta
487 Valley, lost their flat and thick tongues in the recent past.
488 In Aosta Valley Region, the surface area occupied by lakes (1.1 km^2) corresponds to about 0.6% of the area
489 exposed through glacier retreat (179 km^2) over the time period (1850-1991). The total area of modelled
490 overdeepenings (3.1 km^2) corresponds to 1.9% of the remaining glacier area in 1991 (163 km^2). The
491 differences in the values could be attributed to the fact that not all the past overdeepenings are filled with
492 water, originating a lake; the same can happen in the future, especially considering the increase in the
493 amount of debris in glacier basins becoming exposed on slopes, which will likely fill some of the
494 overdeepenings once they become exposed by glacier retreat. The formation of breaches in dams at
495 overdeepenings can also prevent lake formation, as discussed by Colonia et al. (2017). More than a half of
496 the potential overdeepenings are located in the lowest areas of the glaciers and they correspond to the
497 smallest and shallowest elements of the population. The glaciers will probably free the areas where these
498 overdeepenings are located in the coming years. The largest and deepest overdeepenings are located in the
499 accumulation areas of the widest and thickest glaciers of the region (Tribolazione, Rutor, Pre de Bar, Triolet,
500 Grandes Murailles), located in the highest mountain massifs. According to future scenarios, these largest
501 glaciers will probably survive in the coming decades becoming increasingly important with their ice reserves
502 (Zemp et al., 2006; Linsbauer et al., 2012; Zekollari et al., 2019). Hence, the related overdeepenings will not
503 appear very soon but nevertheless probably before the end of the century.
504
505 *5.2 Model performance*
506 Similarly to other authors (Farinotti et al., 2017), in the present study we demonstrated that models
507 inferring ice thickness from surface topography are limited in their ability to reproduce small-scale features
508 of bed topography. Anyway, it should be stated that an accurate simulation of very small glacier lakes is not
509 a crucial demand, because they rarely constitute a hazard or cause relevant issues for environmental
510 management.

A qualitative comparison between modelled overdeepenings and existing lakes shows a good performance of GlabTop2 in terms of location of modelled overdeepenings and lakes, especially for the lakes with area larger than 10,000 m^2 (Figure 12 a, b, c). The model is also able to predict the location of some of the medium size lakes (area between 5,000 and 10,000 m^2) as shown in Figure 12d.

Regarding false negatives, we note that the majority of them is located in steep areas (slope >20°) of small glaciers (surface area <1 km^2). On such glaciers ice thickness in the centre is not much thicker than at the margin, which is a possible reason for this type of "error". Furthermore, and as mentioned above, the model has limited abilities to reproduce small-scale landforms (more than 70% of the false negatives are small lakes, area < 5,000 m^2).

Only two of the 7 false positives are clearly artefacts (ID 13 and ID 14 in Tab. 2 and Fig. 12 e and f). From a geomorphological point of view, they correspond to areas not characterized by a bedrock overdeepening in the real-world, the slope is uniform. They are generated where the glacier surface in the year 1991 was of shallow slope (about 11°), thus likely to result in modelled overdeepenings. However, They are also located very close to the glacier margins where the model often tends to create spurious overdeepenings. The remaining false positives could be real overdeepenings but they are nowadays filled by sediment or dead ice instead of water (e.g.: ID 15, Fig. 5 a). In one case water ponds are currently forming (ID 16, Fig. 5b).

An exception is the Rutor Glacier (Fig. 12a) whose proglacial area features two modelled overdeepenings (ID 2 and ID 5) that are located in the vicinity, but do not overlap, with two actual lakes (M and L_2). This result can be interpreted as an ability of the model in, at least, identifying areas prone to lakes formation.

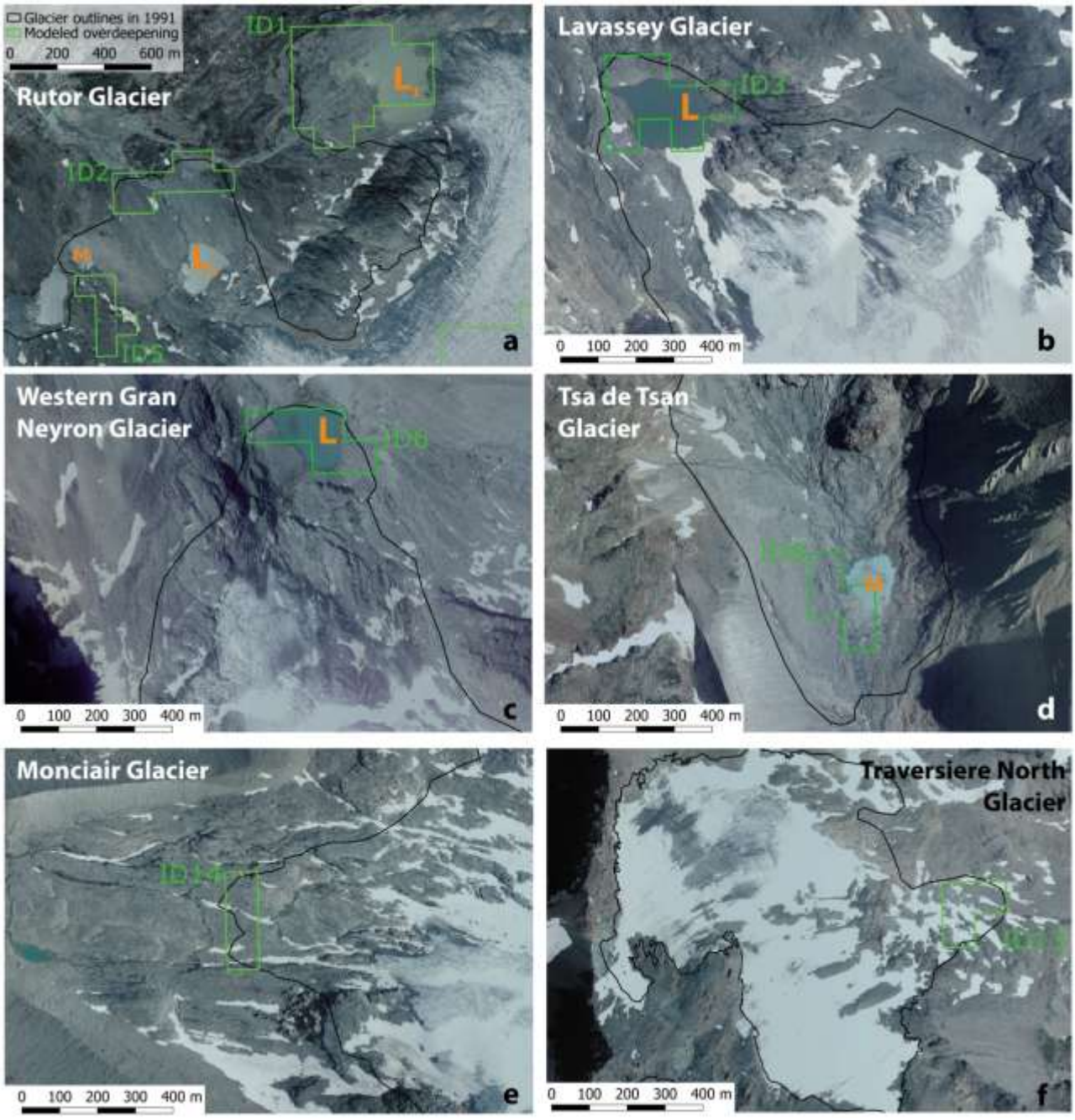

530

531 **Figure 12.** Comparison between the location of modelled overdeepenings (green outlines) and existing
532 large (L) and medium (M) lakes within 1991 glacier extents (black lines) in the study area (a, b, c, d). Panels
533 e and f show examples of model artefacts (false positive). (Imagery: Italian National Geoportal. 2012
534 orthophotos).

535

536 We also compared the location of the modelled overdeepenings with morphological criteria described by
537 Frey et al., 2010a (Fig. 13 a) to identify potential locations of overdeepenings. The reported examples (Fig.

538 13 b, c) show a good correspondence with the three criteria: 1) distinct break in slope; 2) reduction in
539 glacier width; 3) heavily crevassed glacier part below a crevasse-free part. The location of modelled
540 overdeepenings also correspond well with areas with surface slope < 5°, as a first-order criterion for pre-
541 selecting sites with possible overdeepenings (Frey et al., 2010a). We can confirm that the location of the
542 modelled overdeepenings is quite robust while other parameters, like size and depth, are less certain.

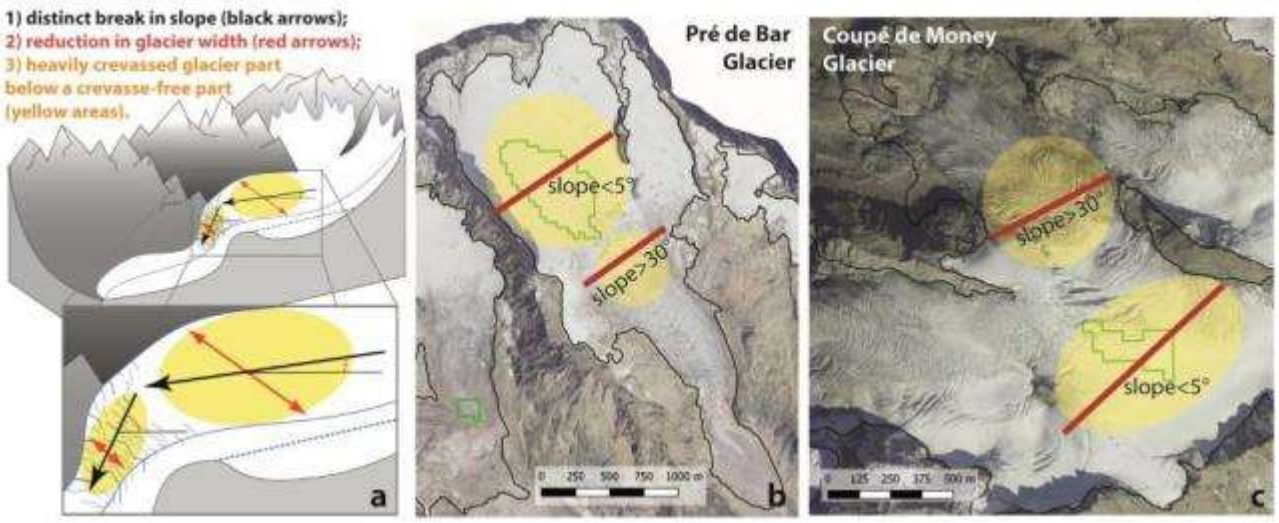

543

544 **Figure 13.** Morphological criteria from Frey et al. (2010a) (a) that indicate the potential existence of glacier-
545 bed overdeepenings for two cases in the study area: Pre de Bar Glacier (b, Mont Blanc Massif) and Coupé
546 de Money Glacier (c, Gran Paradiso Chain). (Imagery: Italian National Geoportal. 2006-07 orthophotos).

547 Some issues in modelling ice thickness and consequently overdeepenings are noticed in the flat and wide
548 areas of the glaciers, as demonstrated in the case of Rutor Glacier (Fig. 8). In such areas, the model might
549 overestimate actual ice thickness. In fact, the Rutor Glacier cannot be defined as a typical valley or
550 mountain glacier, and probably its dynamic is highly influenced by the structural lineaments of the bedrock:
551 these could be the reasons of such divergence between measured and modelled values. In addition, the
552 upper flat (firn) zone is close to a “firn divide” where surface slope becomes zero and the basic assumption
553 of the GlabTop approach (constant basal shear stress) is no longer valid. The differences between GPR data
554 and model results remain unresolved, especially for the site in the lower zone which fulfils all conditions for
555 the formation of an overdeepening according to Frey et al. (2010a). Potential inaccuracies during the
556 acquisition and interpretation of the GPR data have also to be taken into account. In fact, the accuracy in
557 estimating the depth of the interface between ice and bedrock is challenging and depends on several

558 factors such as: morphology of the radiated surface; dielectric permittivity of the ice and its thickness; tilt-
559 angle of the radiation with respect to the inclination of the target; frequency of the radar signal; scattering
560 phenomena due to the presence of heterogeneities in the ice; wave velocity of the ice depending on the ice
561 density. Because of theses challenges in the GPR data acquisition and interpretation, they should always be
562 used with care when validating modelled bed topography.
563
564 *5.3 Backward and forward validation*
565 We believe that the backward approach represents a solid way for validating and evaluating the
566 performance of the model. In particular, the backward approach allows comparing modelled results with
567 real lakes and topography of deglaciated areas. In comparison, GPR data often used for validation (e.g.
568 Farinotti et al. 2017; Frey et al., 2014) can be subjected to large uncertainties because of challenging data
569 acquisition and interpretation (Colonia et al., 2017).
570 Extensive GPR coverage is needed for a good comparison of measured and modelled bedrock because of
571 the large pixel size of the output raster. Short GPR tracks can be used for the validation of the ice thickness
572 at some specific points but they cannot validate the general shape of the bedrock and, in the case of
573 identification of overdeepenings, their real existence. Moreover, analyzing typically linear GPR profiles is
574 challenging because an overdeepening is only fully defined in three dimensions, and the multiple 3D radar
575 reflections imply uncertainties in interpretation. For these reasons, in a GPR survey planning it is necessary
576 to consider the glacier size and shape and the GPR tracks must be long enough in both longitudinal and
577 transversal directions.
578
579 *5.4 Effect of the input data on model results*
580 The spatial resolution of the input DEM influences modelled ice thickness. The smaller the pixel size, the
581 higher the ice thickness, the larger the number of modelled overdeepenings but also the higher the number
582 of false positives. Moreover, as suggested by Paterson (1994) and Haeberli and Hoelzle (1995), the
583 relationship between surface slope and ice thickness is strongest along the central flowline of a glacier and

584 breaks down towards the margins (both laterally and near glacier top and terminus). These issues have to
585 be taken into account in the future implementation of GlabTop2.
586 The comparison between measured and modelled bedrock profiles shows that the morphological variability
587 of the glacier surface (represented by the DEM) is transferred to the modelled bedrock topography
588 because it is calculated by subtraction of modelled ice thickness from the DEM (Paul and Linsbauer, 2012).
589 This explains the better performances, in terms of qualitative agreement, for the high spatial resolution
590 run. Comparing existing lakes with the modelled overdeepenings of the four runs, we found that larger
591 lakes have been well modelled, which confirms the robustness of the model in assessing the location of the
592 overdeepenings and approximately their size.
593 Based on our results, we recommend to choose a medium pixel size (about 60 m) to avoid a great number
594 of false positive and overestimation of ice thickness, overdeepenings number, depth and volume.
595
596 6. CONCLUSIONS
597 The results of the application of the GlabTop2 model to the glaciers of the Aosta Valley Region quantify
598 newest ice volumes for the largest glacierized region of Italy (5.2 ± 1.6 km^3 of total glacier volumes) and the
599 location of potential future glacier lakes (46 potential future overdeepenings covering a total area of 3.1 ±
600 0.9 km^2). Future lake models were missing so far for Italy: therefore, this study fills an important research
601 gap by modelling glacial bed overdeepenings and potential future lakes for the Aosta Valley, the region
602 with the most extensive glacier cover in Italy. Application of this information can be important for the
603 management of water resources and risks related to glacial lakes.
604 The volume of modelled potential future overdeepenings represents only 0.8% of the total modelled glacier
605 volume. We estimate that, continued glacier retreat, will expose mainly smaller and shallower
606 overdeepenings. Larger and deeper geomorphological troughs will remain filled by ice for a few more
607 decades.
608 In addition to the use of well-known methodologies for validation of model of ice thickness and
609 overdeepenings (GPR surveys and morphological criteria), we have proposed a further approach termed

610 “backward approach” that has proven to be useful to compare modelled glacier-bed overdeepenings and
611 real-world landforms. Obviously, GPR surveys remain essential to detect not already exposed
612 overdeepenings but always considering the challenges in the GPR data acquisition and interpretation.
613 Considering the GlabTop approach, we have found that the location of the modelled overdeepeenings is
614 robust while a higher level of uncertainty remains in the dimensions of the overdeepenings.
615 Combining the analysis of the location of modelled lakes with glacier retreat scenarios will allow to define
616 the approximate year or decade during which the potential lakes will appear (Colonia et al., 2017).
617 To our knowledge, overdeepenings underneath Italian glaciers have not yet been modelled. Extending the
618 modelling to the rest of the Italian Alps would be important for estimating the total amount of water stored
619 in the future lakes and for understanding how the alpine environment will look in the future, following
620 continued glacier shrinkage.

Declaration of competing interest

The authors declare that they have no known competing financial interests or personal relationships that could have appeared to influence the work reported in this paper.

Acknowledgments

The authors acknowledge Umberto Morra di Cella (ARPA Valle d'Aosta) for sharing GPR data of the Gran Etret Glacier and Andrea Tamburini and Fabio Villa (IMAGEO S.r.l.) for those of the Rutor Glacier. Moreover, a special thank to Nicola Colombo and Arnoldo Welf for their technical support in the GPR survey at Indren Glacier in September 2016. The authors are furthermore grateful towards the two anonymous reviewers and Holger Frey for constructive reviews that substantially improved the manuscript.

This research did not receive any specific grant from funding agencies in the public, commercial, or not-for-profit sectors.

633 REFERENCES

634 Ajassa, R., Biancotti, A., Biasini, A., Brancucci, G., Caputo, C., Pugliese, F. Salvatore, M.C., 1994. Il catasto dei
635 ghiacciai italiani: primo confronto tra i dati 1958 e 1989. Il Quaternario 7 (1), 497-502,
636 http://www.aiqua.it/en/index.php/volume-7-1-b/782-il-catasto-dei-ghiacciai-italiani-primo-
637 confronto-tra-i-dati-1958-e-1989/file.

638 Ajassa, R., Biancotti, A., Biasini, A., Brancussi, G., Carton, A., Salvatore M. C., 1997. Changes in the number
639 and area of Italian Alpine glaciers between 1958 and 1989. Geogr. Fis. Dian. Quat. 20, 293-297,
640 http://www.glaciologia.it/wp-
641 content/uploads/FullText/full_text_20_2/16_GFDQ_20_2_Ajassa_293_297.pdf.

642 Allen, S.K., Schneider, D., Owens, I.F., 2009. First approaches towards modelling glacial hazards in the
643 Mount Cook region of New Zealand's Southern Alps. Nat. Hazards Earth Syst. Sci. 9, 481-499,
644 https://doi.org/10.5194/nhess-9-481-2009.

645 Bolch, T., Buchroithner, M.F., Peters, J., Baessler, M., Bajracharya, S., 2008. Identification of glacier motion
646 and potentially dangerous glacial lakes in the Mt. Everest region/Nepal using spaceborne imagery.
647 Nat. Hazards Earth Syst. Sci. 8, 1329-1340, https://doi.org/10.5194/nhess-8-1329-2008.

648 Bolch, T., Peters, J., Yegorov, A., Pradhan, B., Buchroithner, M., Blagoveschchensky, V., 2011. Identification
649 of potentially dangerous glacial lakes in the northern Tien Shan. Nat. Hazards 59 (3), 1691-1714,
650 https://doi.org/10.1007/s11069-011-9860-2.

651 Bolch, T., Kulkarni, A., Kääb, A., Huggel, C., Paul, F., Cogley, J.G., Frey, H., Kargel, J.S., Fujita, K., Scheel, M.,
652 Bajracharya, S., Stoffel, M., 2012. The State and Fate of Himalayan Glaciers. Science 336 (6079),
653 310-314, DOI: 10.1126/science.1215828.

654 Buckel, J., Otto, J.C., Prasicek, G., Keuschnig, M., 2018. Glacial lakes in Austria - Distribution and formation
655 since the Little Ice Age. Global Planet. Change 164, 39-51,
656 https://doi.org/10.1016/j.gloplacha.2018.03.003.

657 Capps, D.M., Clague, J.J., 2014. Evolution of glacier-dammed lakes through space and time; Brady Glacier,
658 Alaska, USA. Geomorphology 210, 59-70, https://doi.org/10.1016/j.geomorph.2013.12.018.

659 Carrivick, J.L., Tweed, F.S., 2013. Proglacial lakes: character, behavior and geological importance.
660 Quaternary Sci. Rev. 78, 34-52, https://doi.org/10.1016/j.quascirev.2013.07.028.
661 CGI-CNR – Comitato Glaciologico Italiano & Consiglio Nazionale delle Ricerche, 1961. Catasto dei Ghiacciai
662 Italiani, Anno Geofisico Internazionale 1957-1958. Ghiacciai del Piemonte. Comitato Glaciologico
663 Italiano, Torino, 2, 324 pp.
664 Čiamporová-Zaťovičová, Z., Čiampor, F., 2017. Alpine lakes and ponds - a promising source of high genetic
665 diversity in metapopulations of aquatic insects. Inland Waters 7 (1), 109-117,
666 https://doi.org/10.1080/20442041.2017.1294361.
667 Citterio, M., Diolaiuti, G.A., Smiraglia, C., D'Agata, C., Carnielli, T., Stella, G., Siletto, G.B., 2007. The
668 fluctuations of Italian glaciers during the last century: a contribution to knowledge about alpine
669 glacier changes. Geogr. Ann. A 89 (3), 164-1821, https://doi.org/10.1111/j.1468-
670 0459.2007.00316.x.
671 Colonia, D., Torres, J., Haeberli, W., Schauwecker, S., Braendle, E., GIraldez, C,. Cochachin, A., 2017.
672 Compiling an Inventory of Glacier-Bed Overdeepenings and Potential New Lakes in De-Glaciating
673 Areas of the Peruvian Andes: Approach, First Results, and Perspectives for Adaptation to Climate
674 Change. Water 9 (5), 336, https://doi.org/10.3390/w9050336.
675 Diolaiuti, G.A., Citterio, M., Carnielli, T., D'agata, C., Kirkbride, M., Smiraglia, C., 2006. Rates, processes and
676 morphology of fresh-water calving at Miage Glacier (Italian Alps). Hydrol. Process. 20, 2233-2244,
677 https://doi.org/10.1002/hyp.6198.
678 Diolaiuti, G., Smiraglia, C., 2010. Changing glaciers in a changing climate: how vanishing geomorphosites
679 have been driving deep changes in mountain landscapes and environments. Géomorphologie 16
680 (2), 131-152, DOI 10.4000/geomorphologie.7882.
681 Diolaiuti, G.A., Bocchiola, D., Vagliasindi, M., D'Agata, C., Smiraglia, C., 2012. The 1975-2005 glacier changes
682 in Aosta Valley (Italy) and the relations with climate evolution. Prog. Phys. Geog. 36 (6), 764-785,
683 https://doi.org/10.1177/0309133312456413.

684 Drenkhan, F., Guardamino, L., Huggel, C,. Frey, H., 2018. Current and future glacier and lake assessment in
685 the deglaciating Vilcanota-Urubamba basin, Peruvian Andes. Global Planet. Change 169, 105-118,
686 https://doi.org/10.1016/j.gloplacha.2018.07.005.
687 Drenkhan, F., Huggel, C., Guardamino, L., Haeberli, W., 2019. Managing risks and future options from new
688 lakes in the deglaciating Andes of Peru: The example of the Vilcanota-Urubamba basin. Sci. Total
689 Environ. 665, 465-483, https://doi.org/10.1016/j.scitotenv.2019.02.070.
690 Dutto, F., Mortara, G., 1992. Rischi connessi con la dinamica glaciale nelle Alpi Italiane. Geogr. Fis. Din.
691 Quat. 15, 85-99, http://www.glaciologia.it/wp-
692 content/uploads/FullText/full_text_15_1_2/11_GFDQ_15_1_2_Dutto_85_99.pdf.
693 Emmer, A., Vilímek, V., Klimeš, J., Cochachin, A., 2014. Glacier retreat, lakes development and associated
694 natural hazards in Cordilera Blanca, Peru, in: Shan, W., Guo, Y., Wang, F., Marui, H., Strom, A. (Eds.),
695 Landslides in Cold Regions in the Context of Climate Change. Environmental Science and
696 Engineering, Springer, Cham, 231-252, https://doi.org/10.1007/978-3-319-00867-7_17.
697 Emmer, A., Merkl, S., Mergili, M., 2015. Spatiotemporal patterns of high-mountain lakes and related
698 hazards in western Austria. Geomorphology 246, 602-616,
699 https://doi.org/10.1016/j.geomorph.2015.06.032.
700 Emmer, A., Klimeš, J., Mergili, M., Vilímek, V., Cochachin, A., 2016. 822 lakes of the Cordillera Blanca: An
701 inventory, classification, evolution and assessment of susceptibility to outburst floods. Catena 147,
702 269-279, https://doi.org/10.1016/j.catena.2016.07.032.
703 Farinotti, D., Huss, M., Bauder, A., Funk, M., Truffer, M., 2009. A method to estimate the ice volume and
704 ice-thickness distribution of alpine glaciers. Journal of Glaciology 55 (191), 422-430,
705 https://doi.org/10.3189/002214309788816759.
706 Farinotti, D., Brinkerhoff, D.J., Clarke, G.K.C., Fürst, J.J., Frey, H., Gantayat, P., Gillet-Chaulet, F., Girard, C.,
707 Huss, M., Leclercq, P. W., Linsbauer, A., Machguth, H., Martin, C., Maussion, F., Morlighem, M.,
708 Mosbeux, C., Pandit, A., Portmann, A., Rabatel, A., Ramsankaran, R., Reerink, T.J., Sanchez, O.,
709 Stentoft, P.A., Singh Kumari, S., van Pelt, W.J.J., Anderson, B., Benham, T., Binder, D., Dowdeswell,

J.A., Fischer, A., Helfricht, K., Kutuzov, S., Lavrentiev, I., McNabb, R., Gudmundsson, G.H., Li, H., Andreassen, L.M., 2017. How accurate are estimates of glacier ice thickness? Results from ITMIX, the Ice Thickness Models Intercomparison eXperiment. Cryosphere 11, 949-970, https://doi.org/10.5194/tc-11-949-2017.

Fischer, U.H., Haeberli, W., 2012. Overdeepenings in Glacial Systems: Processes and Uncertainties. Eos 93 (35), 341-341, https://doi.org/10.1029/2012EO350010.

FMS – Fondazione Montagna Sicura, 2016. Bilancio sociale e di Missione 2016, 68 pp, http://www.fondazionemontagnasicura.org/eventi/bilancio-sociale-e-di-missione-2016.

Frey, H., Haeberli, W., Linsbauer, A., Huggel, C., Paul, F., 2010a. A multi-level strategy for anticipating future glacier lake formation and associated hazard potential. Nat. Hazard. Earth Sys. 10, 339-352, https://doi.org/10.5194/nhess-10-339-2010.

Frey, H., Huggel, C., Paul, F., Haeberli, W., 2010b. Automated detection of glacier lakes based on remote sensing in view of assessing associated hazard potentials, in: Kaufmann, V., Sulzer, W. (Eds.), Proceedings of the 10th International Symposium on High Mountain Remote Sensing Cartography. Grazer Schriften der Geographie und Raumfoschung 45, 261-272.

Frey, H., Machguth, H., Huss, M., Huggel, C., Bajracharya, S., Bolch, T., Kulkarni, A., Linsbauer, A., Salzmann, N., Stoffel, M., 2014. Estimating the volume of glaciers in the Himalayan–Karakoram region using different methods. Cryosphere 8, 2313-2333, https://doi.org/10.5194/tc-8-2313-2014.

Galluccio, A., 1998. I nuovi laghi proglaciali lombardi. Terra glacialis 1, 133-151, http://lnx.servizioglaciologicolombardo.it/index.php/pubblicazioni/terra-glacialis/347-01-terra-glacialis-nd-1.

Gardelle, J., Arnaud, Y., Berthier, E., 2011. Contrasted evolution of glacial lakes along the Hindu Kush Himalaya mountain range between 1990 and 2009. Global Planet. Change 75 (1-2), 47-55, https://doi.org/10.1016/j.gloplacha.2010.10.003.

Giardino, M., Mortara, G., Chiarle, M., 2017. The glaciers of the Valle d'Aosta and Piemonte Regions: Records of Present and Past Environmental and Climate Change, in: Soldati, M., Marchetti, M.

(Eds), Landscapes and Landforms of Italy. World Geomorphological Landscapes, Springer, Cham, 77-88, https://doi.org/10.1007/978-3-319-26194-2_6.

Haeberli, W., Hoelzle, M., 1995. Application of inventory data for estimating characteristics of and regional climate-change effects on mountain glaciers: a pilot study with the European Alps. Ann. Glaciol. 21, 206-212, https://doi.org/10.3189/S0260305500015834.

Haeberli, W., Buetler, M., Huggel, C., Lehmann Friedli, T., Schaub, Y., Schleiss, A J., 2016a. New lakes in deglaciating high-mountain regions – opportunities and risks. Climatic Change 139 (2), 202-214, https://doi.org/10.1007/s10584-016-1771-5.

Haeberli, W., Linsbauer, A., Cochachin, A., Salazar, C., Fischer, U.H., 2016b. On the morphological characteristics of overdeepenings in high-mountain glacier beds. Earth Surf. Proc. Land. 41, 1980-1990, https://doi.org/10.1002/esp.3966.

Hanshaw, M.N., Bookhagen, B., 2014. Glacial areas, lake areas, and snow lines from 1975 to 2012: status of the Cordillera Vilcanota, including the Quelccaya Ice Cap, northern central Andes, Peru. Cryosphere 8, 359-376, https://doi.org/10.5194/tc-8-359-2014.

Helfricht, K., Huss, M., Fischer, A., Otto J-C, 2019. Calibrated Ice Thickness Estimate for All Glaciers in Austria. Front. Earth Sci. 7, 68, https://doi.org/10.3389/feart.2019.00068.

Huggel, C., Kääb, A., Haeberli, W., Teysseire, P., Paul, F., 2002. Remote sensing based assessment of hazards from Glacier lake outbursts: a case study in the Swiss Alps. Can. Geotech. J. 39 (2), 316-330, https://doi.org/10.1139/t01-099.

Huss, M., Farinotti, D., 2012. Distributed ice thickness and volume of all glaciers around the globe. J. Geophys. Res. 117, F04010. doi:10.1029/2012JF002523.

IPCC, 2013. Climate Change 2013: The Physical Science Basis. Contribution of Working Group I to the Fifth Assessment Report of the Intergovernmental Panel on Climate Change. Cambridge University Press, Cambridge, 1535 pp, https://doi.org/10.1017/CBO9781107415324.

Kapitsa, V., Shahgedanova, M., Machguth, H., Severskiy, I., Medeu, A., 2017. Assessment of evolution and risks of glacier lake outbursts in the Djungarskiy Alatau, Central Asia, using Landsat imagery and

762 glacier bed topography modelling. Nat. Hazards Earth Syst. Sci. 17 (10), 1837-1856,
763 https://doi.org/10.5194/nhess-17-1837-2017.
764 Komori, J., 2008. Recent expansions of glacial lakes in the Bhutan Himalayas. Quatern. Int. 184 (1), 177-186,
765 https://doi.org/10.1016/j.quaint.2007.09.012.
766 Linsbauer, A., Paul, F., Hoelzle, M., Frey, H., Haeberli, W., 2009. The Swiss Alps Without Glaciers – A GIS-
767 based Modelling Approach for Reconstruction of Glacier Beds, in: Purves, R., Gruber, S., Straumann,
768 R., Hengl, T. (Eds.), Proceedings of Geomorphometry 2009, 243-247,
769 http://geomorphometry.org/system/files/linsbauer2009geomorphometry.pdf.
770 Linsbauer, A., Paul, F., Haeberli, W., 2012. Modeling glacier thickness distribution and bed topography over
771 entire mountain ranges with GlabTop: Application of a fast and robust approach. J. Geophys. Res.
772 117, F03007, https://doi.org/10.1029/2011JF002313.
773 Linsbauer, A., Frey, H., Haeberli, W., Machguth, H., Azam, M.F., Allen, S., 2016. Modelling glacier-bed
774 overdeepenings and possible future lakes for glaciers in the Himalaya-Karakoram region. Ann.
775 Glaciol. 57 (71), 119-130, https://doi.org/10.3189/2016AoG71A627.
776 Loriaux, T., Casassa, G., 2012. Evolution of glacial lakes from the Northern Patagonia Icefield and terrestrial
777 water storage in a sea-level rise context. Global Planet. Change 102, 33-40,
778 https://doi.org/10.1016/j.gloplacha.2012.12.012.
779 Magnin, F., Haeberli, W., Linsbauer, A., Deline, P., Ravanel, L., 2020. Estimating glacier-bed overdeepenings
780 as possible sites of future lakes in the de-glaciating Mont Blanc massif (Western European Alps).
781 Geomorphology 350, 106913, https://doi.org/10.1016/j.geomorph.2019.106913.
782 Mergili, M., Müller, J.P., Schneider, J.F., 2013. Spatio-temporal development of high-mountain lakes in the
783 headwaters of the Amu Darya River (Central Asia). Global Planet. Change 107, 13-24,
784 https://doi.org/10.1016/j.gloplacha.2013.04.001.
785 Orombelli, G., 2005. Il Ghiacciaio del Rutor (Valle d'Aosta) nella Piccola Età Glaciale. Geogr. Fis. Dian. Quat.
786 Suppl. VII, 239-251,

787 http://www.glaciologia.it/wp-
788 content/uploads/Supplementi/Abstracts/Abstract_SGFDQ_VII_2005/28_SGFDQ_VII_Orombelli_Ab
789 st.pdf.
790 Orombelli, G., 2011. Holocene mountain glacier fluctuations: A global overview. Geogr. Fis. Dian. Quat.
791 34(1), 17-24, DOI 10.4461/GFDQ.2011.34.2.
792 Paterson, W.S.B., 1994. The Physics of Glaciers. Elsevier, 480 pp, https://doi.org/10.1016/C2009-0-14802-X.
793 Paul, F., Kääb, A., Haeberli, W., 2007. Recent glaciers changes in the Alps observed by satellite:
794 consequences for future monitoring strategies. Global Planet. Change 56 (1-2), 111-122,
795 https://doi.org/10.1016/j.gloplacha.2006.07.007.
796 Paul, F., Linsbauer, A., 2012. Modeling of glacier bed topography from glacier outlines, central branch lines,
797 and a DEM. Int. J. Geogr. Inf. Sci. 26 (7), 1173-1190,
798 https://doi.org/10.1080/13658816.2011.627859.
799 Purdie, H., 2013. Glacier Retreat and Tourism: Insights from New Zealand. Mt. Res. Dev. 33(4), 463-472,
800 https://doi.org/10.1659/MRD-JOURNAL-D-12-00073.1.
801 Reynard, E., 2004. Geosites, in: Goudie, A.S. (Ed), Encyclopedia of Geomorphology. London, Routledge, 440,
802 https://doi.org/10.4324/9780203381137.
803 Roberti, G., Ward, B., van Wyk de Vries B., Friele, P., Perotti, L., Clague, J.J., Giardino, M., 2018. Precursory
804 slope distress prior to the 2010 Mount Meager landslide, British Columbia. Landslides 15 (4), 637-
805 647, https://doi.org/10.1007/s10346-017-0901-0.
806 Salerno, F., Thakuri, S., D'Agata, C., Smiraglia, C., Manfredi, E.C., Viviano, G., Tartari, G., 2012. Glacial lake
807 distribution in the Mount Everest region: Uncertainty of measurement and conditions of formation.
808 Global Planet. Change 92-93, 30-39, https://doi.org/10.1016/j.gloplacha.2012.04.001.
809 Salerno, F., Gambelli, S., Viviano, G., Thakuri, S., Guyennon, N., D'agata, C., Diolaiuti, G., Smiraglia, C.,
810 Stefani, F., Bocchiola, D., Tartari, G., 2014. High alpine ponds shift upwards as average
811 temperatures increase: A case study of the Ortles-Cevedale mountain group (Southern Alps, Italy)

over the last 50 years. Global Planet. Change 120, 81-91, https://doi.org/10.1016/j.gloplacha.2014.06.003.

Salerno, F., Thakuri, S., Guyennon, N., Viviano, G., Tartari, G., 2016. Glacier melting and precipitation trends detected by surface area changes in Himalayan ponds. Cryosphere 10, 1433-1448, https://doi.org/10.5194/tc-10-1433-2016.

Salvatore, M.C., Zanoner, T., Baroni, C., Carton, A., Banchieri, F.A., Viani, C., Giardino, M., Perotti, L., 2015. The state of Italian glaciers: a snapshot of the 2006-2007 hydrological period. Geogr. Fis. Dian. Quat. 38 (2), 175-198, DOI 10.4461/GFDQ.2015.38.16.

Schomacker, A., 2010. Expansion of ice-marginal lakes at the Vatnajökull ice cap, Iceland, from 1999 to 2009. Geomorphology 119 (1-2), 232-236, https://doi.org/10.1016/j.geomorph.2010.03.022.

Smiraglia, C., Azzoni, R.S., D'agata, C., Maragno, D., Fugazza, D., Diolaiuti, G.A., 2015. The evolution of the Italian glaciers from the previous data base to the New italian Inventory. Preliminary considerations and results. Geogr. Fis. Dian. Quat. 38 (1), 79-87, DOI 10.4461/GFDQ.2015.38.08.

Stokes, C.R., Popovnin, V., Aleynikov, A., Gurney, S.D., Shahgedanova, M., 2007. Recent glacier retreat in the Caucasus Mountains, Russia, and associated increase in supraglacial debris cover and supra-/proglacial lake development. Ann. Glaciol. 46, 195-203, https://doi.org/10.3189/172756407782871468.

Tartari, G, Salerno, F., Buraschi, E., Bruccoleri, C., Smiraglia, C., 2008. Lake surface area variations in the North-Eastern sector of Sagarmatha National Park (Nepal) at the end of the 20th Century by comparison of historical maps. J. Limnol. 67 (2), 139-154, https://doi.org/10.4081/jlimnol.2008.139.

Terrier, S., Jordan, F., Schleiss, A.J., Haeberli, W., Hugge,l C., Künzler, M., 2011. Optimized and adapted hydropower management considering glacier shrinkage scenarios in the Swiss Alps, in: Schleiss, A, Boes, R.M. (Eds.), Proceedings of the International Symposium on Dams and Reservoirs under Changing Challenges. Taylor & Francis Group, 497-508, http://infoscience.epfl.ch/record/167089/files/2011-

774_Terrier_Jordan_Schleiss_Haeberli_Huggel_Kunzler_Optimized_and_adapted_hydropower_management_considering_glacier_shrinkage_scenarios_in_the_swiss_alps.pdf

Tiberti, R., Buscaglia, F., Callieri, C., Rogora, M., Tartari, G, Sommaruga, R., 2019. Food Web Complexity of High Mountain Lakes is Largely Affected by Glacial Retreat. Ecosystems 1-14, https://doi.org/10.1007/s10021-019-00457-8.

[dataset] Viani, C., 2018. Inventories of glacier lakes in the Western Italian Alps from the 1930s to 2012. PANGAEA, https://doi.org/10.1594/PANGAEA.896023.

Viani, C., Giardino, M., Huggel, C., Perotti, L., Mortara, G., 2016. An overview of glacier lakes in the Western Italian Alps from 1927 to 2014 based on multiple data sources (historical maps, orthophotos and reports of the glaciological surveys). Geogr. Fis. Dian. Quat. 39 (2), 203-214, DOI 10.4461/GFDQ.2016.39.19.

Villa, F., De Amicis, M., Maggi V., 2007. GIS analysis of Rutor glacier (Aosta Valley) volume and terminus variations. Geogr. Fis. Dian. Quat. 30, 87-95, http://www.glaciologia.it/wp-content/uploads/FullText/full_text_30_1/09_Villa_87-95.pdf.

Villa, F., Tamburini, A., Deamici,s M., Sironi, S., Maggi, V., Rossi, G., 2008. Volume decrease of Rutor Glacier (Western Italian Alps) since Little Ice Age: a quantitative approach combining GPR, GPS and cartography. Geogr. Fis. Dian. Quat. 31, 63-70, http://www.glaciologia.it/wp-content/uploads/FullText/full_text_31_1/08_Villa_63_70.pdf.

Wessels, R., Kargel, J.S., Kieffer, H.H., 2002. ASTER measurement of supraglacial lakes in the Mount Everest region of the Himalaya. Ann. Glaciol. 34, 399-408, https://doi.org/10.3189/172756402781817545.

Worni, R., Huggel, C., Stoffel, M., 2013. Glacier lakes in the Indian Himalayas – From an area-wide glacial lake inventory to on-site and modeling based risk assessment of critical glacial lakes. Sci. Total Environ. 468-469, Suppl., S71-84, https://doi.org/10.1016/j.scitotenv.2012.11.043.

Zekollari, H., Huss, M., Farinotti, D., 2019. Modelling the future evolution of glaciers in the European Alps under the EURO-CORDEX RCM ensemble. Cryosphere 13, 1125-1146, https://doi.org/10.5194/tc-13-1125-2019.

Zemp, M., Haeberli, W., Hoelzle, M. Paul, F., 2006. Alpine glaciers to disappear within decades? Geophys. Res. Lett. 33 (13), L13504, https://doi.org/10.1029/2006GL026319.

Zhang G., Yao T., Xie H., Wang W., Yang W., 2015. An inventory of glacial lakes in the Third Pole region and their changes in response to global warming. Global Planet. Change 131, 148-157, https://doi.org/10.1016/j.gloplacha.2015.05.013.

Zhang, G., Yao, T., Piao, S., Bolch, T., Xie, H., Chen, D., Gao, Y., O'Reilly, C.M., Shum, C.K., Yang, K., Yi, S., Lei, Y., Wang, W., He, Y., Shang, K., Yang, X., Zhang, H., 2017. Extensive and drastically different alpine lake changes on Asia's high plateaus during the past four decades. Geophys. Res. Lett. 44 (1), 252-260, https://doi.org/10.1002/2016GL072033.